Numerical evaluation of the equivalent properties of Macro Fiber Composite (MFC) transducers using periodic homogenization

Arnaud Deraemaeker[a], Houssein Nasser[b]

[a] *Université Libre de Bruxelles - BATir, 50 av F.D. Roosevelt, CP 194/02, B-1050 Brussels*
[b] *CRP Henri Tudor, 29 Avenue John F. Kennedy, L-1855 Luxembourg*

Abstract

This paper focuses on the evaluation of the homogeneous properties of the active layer in Macro Fiber Composite (MFC) transducers using finite element periodic homogenization. The proposed method is applied to both d_{31} and d_{33} MFCs and the results are compared to previously published analytical mixing rules, showing a good agreement. The main advantages of the finite element homogenization is the possibility to take into account local details in the representative volume element such as complicated electrode patterns or local variations of the poling direction due to curved electric field lines. Although these influences have been found to be rather small in the present study, the method presented is useful for a better understanding of the behavior of piezocomposite transducers.

Keywords: Piezoelectric material, piezocomposite transducer, Macro Fiber Composite (MFC), Periodic homogenization, finite element method

1. Introduction

1.1. Piezocomposite transducers

Thin piezoelectric actuators and sensors are used in a variety of applications such as active vibration control, structural health monitoring or shape control. In these applications, PZT ceramics are commonly used due to their relatively low cost, high bandwidth and good actuation capabilities. The major drawbacks of these ceramics are their brittleness and very low flexibility. This problem can be overcome using piezocomposite transducers in which

piezoelectric fibers are mixed with a softer passive epoxy matrix. A typical piezocomposite transducer is made of an active layer sandwiched between two soft thin encapsulating layers (Figure 1). The packaging plays two different roles: (i) applying prestress to the active layer in order to avoid cracks, and (ii) bringing the electric field to the active layer through the use of a specific surface electrode pattern. The electrodes can be either continuous, in which case a voltage difference is applied between the top and bottom electrodes resulting in an electric field perpendicular to the plane of the transducer, or interdigitated [1], resulting in a curved electric field mostly aligned in the direction of the fibers (Figure 2). In the first case, the piezoelectric fibers are driven in the d_{31} mode, while in the second case, the fibers are driven in the d_{33}-mode, resulting in a higher achievable free strain but for much higher applied voltages. In the family of piezocomposite transducers, there exist many different types, differing mainly in the electrode configuration and the type of active layer which can consist of a bulk ceramic [2, 3, 4], large square [5] or round fibers [6], or even small fibers (see for example [7] and [8] for a review of these different types of piezocomposites).

Round fibers are usually not very effective due to the problem of dielectric permittivity mismatch which forces the electrodes to be in direct contact with the active fibers. For this reason and also for reasons linked to the manufacturing, the most successful implementation of piezocomposite transducers is probably the Macro Fiber Composites (MFC) manufactured and sold by the company *Smart Material*. Both d_{31} and d_{33} actuators and sensors have been developed and are currently sold.

In general, for a correct design of active vibration control or structural health monitoring systems, it is useful to develop numerical models (i.e. finite element models) of the structure equipped with piezoelectric transducers. For thin plate-like structures, three-dimensional volume finite elements should be avoided and an adequate approach is the use of multi-layer shell elements including piezoelectric layers [9]. Such elements are available in commercial finite element softwares such as SAMCEF (http://www.samcef.com) or the *Structural Dynamics Toolbox (SDT)* (http://www.sdtools.com) under *Matlab*. In this approach, the active layer is not modeled in details, but by an homogeneous active layer for which the equivalent properties need to be known. Unfortunately, the information found in the datasheet is not sufficient to determine all the mechanical, dielectric and piezoelectric equivalent

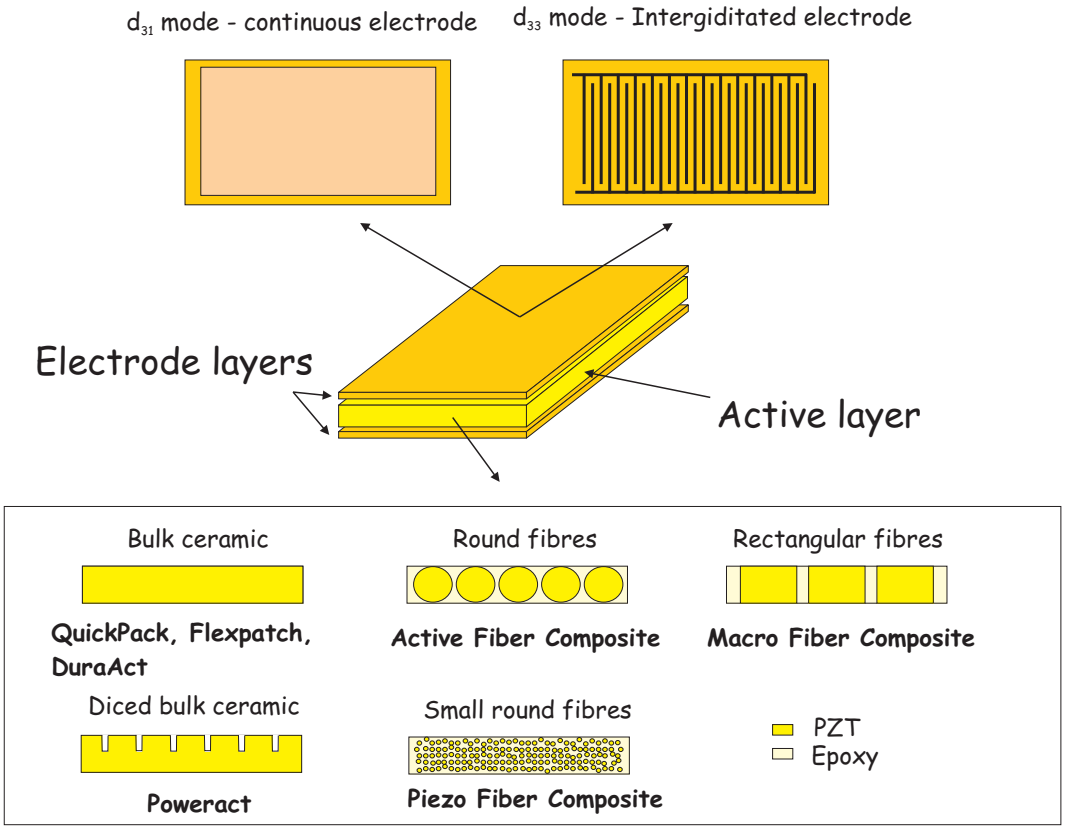

Figure 1: Overview of flat piezocomposite transducers with surface electrodes

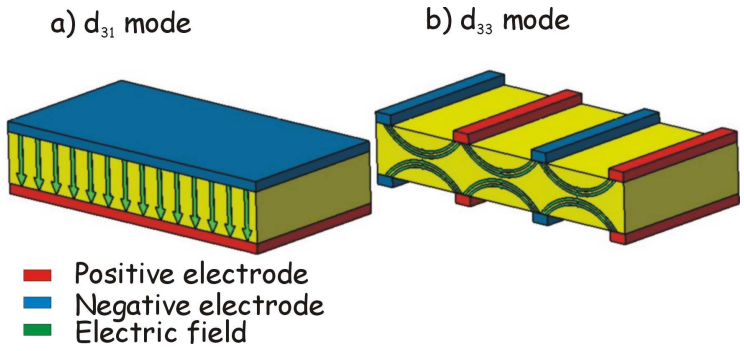

Figure 2: Electric field distribution for different electrode configurations

properties. This was the reason for the development of mixing rules for the determination of the equivalent properties of MFCs from the properties of the constituents in [10]. The mixing rules were derived using the uniform field method and compared to numerical results obtained using the method described and discussed in more details here.

In this paper, after introducing the properties of homogeneous piezoelectric active layers under plane stress driven either in the d_{31} or the d_{33} mode, we develop a numerical method for the evaluation of the equivalent mechanical, piezoelectric and dielectric properties of piezocomposite transducers. The method is based on numerical periodic homogenization performed on a representative volume element (RVE) using three-dimensionnal coupled piezoelectric finite elements. It differs from the methods generally presented in the literature **(see for example [24, 20])** in three aspects: (i) the real electrode configuration and the resulting equipotential conditions are taken into account in the RVE, (ii) the peridocicity condition is enforced only in the plane of the transducer, due to the size of the fibers which is of the same order of magnitude as the thickness of the transducer, and (iii) the poling vector is not constant in the RVE and follows the potentially curved electric field lines resulting from the real electrodes configuration.

The method is applied to both d_{31} and d_{33} MFCs with different volume fractions of fibers and the results are compared to the analytical results using the mixing rules developed in [10]. For d_{33} MFCs, the influence of the curved electric field lines as well as the direction of polarization vector on the homogeneous properties are discussed in details.

1.2. Constitutive equations of piezocomposite transducers

Using the standard IEEE notations for linear piezoelectricity, the constitutive equations for an orthotropic piezoelectric material are given by:

$$\begin{Bmatrix} T_1 \\ T_2 \\ T_3 \\ T_4 \\ T_5 \\ T_6 \\ D_1 \\ D_2 \\ D_3 \end{Bmatrix} = \begin{bmatrix} c_{11}^E & c_{12}^E & c_{13}^E & 0 & 0 & 0 & 0 & 0 & -e_{31} \\ c_{12}^E & c_{22}^E & c_{23}^E & 0 & 0 & 0 & 0 & 0 & -e_{32} \\ c_{13}^E & c_{23}^E & c_{33}^E & 0 & 0 & 0 & 0 & 0 & -e_{33} \\ 0 & 0 & 0 & c_{44}^E & 0 & 0 & 0 & -e_{24} & 0 \\ 0 & 0 & 0 & 0 & c_{55}^E & 0 & -e_{15} & 0 & 0 \\ 0 & 0 & 0 & 0 & 0 & c_{66}^E & 0 & 0 & 0 \\ 0 & 0 & 0 & 0 & e_{15} & 0 & \varepsilon_{11}^S & 0 & 0 \\ 0 & 0 & 0 & e_{24} & 0 & 0 & 0 & \varepsilon_{22}^S & 0 \\ e_{31} & e_{32} & e_{33} & & 0 & 0 & 0 & 0 & \varepsilon_{33}^S \end{bmatrix} \begin{Bmatrix} S_1 \\ S_2 \\ S_3 \\ S_4 \\ S_5 \\ S_6 \\ E_1 \\ E_2 \\ E_3 \end{Bmatrix} \tag{1}$$

where E_i and D_i are the components of the electric field vector and the electric displacement vector, and T_i and S_i are the components of stress and strain vectors, defined according to:

$$\begin{Bmatrix} T_1 \\ T_2 \\ T_3 \\ T_4 \\ T_5 \\ T_6 \end{Bmatrix} = \begin{Bmatrix} T_{11} \\ T_{22} \\ T_{33} \\ T_{23} \\ T_{13} \\ T_{12} \end{Bmatrix} \qquad \begin{Bmatrix} S_1 \\ S_2 \\ S_3 \\ S_4 \\ S_5 \\ S_6 \end{Bmatrix} = \begin{Bmatrix} S_{11} \\ S_{22} \\ S_{33} \\ 2\,S_{23} \\ 2\,S_{13} \\ 2\,S_{12} \end{Bmatrix} \tag{2}$$

1.2.1. d_{31} - piezocomposites

For d_{31} piezocomposites, the poling direction (conventionally direction 3) is normal to the plane of the patches (Figure 3a) and according to the plane stress assumption $T_3 = 0$. The electric field is assumed to be aligned with the polarization vector ($E_2 = E_1 = 0$). The constitutive equations reduce to:

$$\begin{Bmatrix} T_1 \\ T_2 \\ T_4 \\ T_5 \\ T_6 \\ D_3 \end{Bmatrix} = \begin{bmatrix} c_{11}^{E*} & c_{12}^{E*} & 0 & 0 & 0 & -e_{31}^* \\ c_{12}^{E*} & c_{22}^{E*} & 0 & 0 & 0 & -e_{32}^* \\ 0 & 0 & c_{44}^{E*} & 0 & 0 & 0 \\ 0 & 0 & 0 & c_{55}^{E*} & 0 & 0 \\ 0 & 0 & 0 & 0 & c_{66}^{E*} & 0 \\ e_{31}^* & e_{32}^* & 0 & 0 & 0 & \varepsilon_{33}^{S*} \end{bmatrix} \begin{Bmatrix} S_1 \\ S_2 \\ S_4 \\ S_5 \\ S_6 \\ E_3 \end{Bmatrix} \tag{3}$$

where the superscript * denotes the properties under the plane stress assumption (which are not equal to the properties in 3D). The constitutive equations can be written in a matrix form, separating the mechanical and

the electrical parts:

$$\{T\} = \left[c^{E*}\right]\{S\} - [e^*]^T\{E\}$$
$$\{D\} = [e^*]\{S\} + \left[\varepsilon^{S*}\right]\{E\}$$

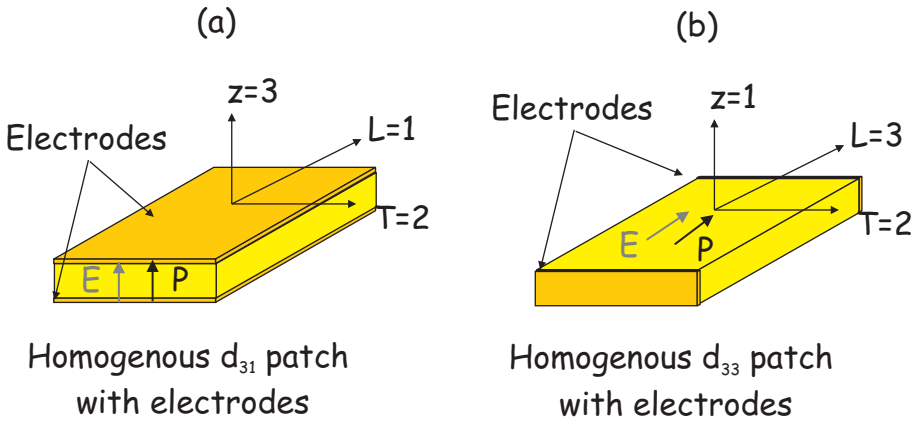

Figure 3: Homogeneous models of the piezoelectric layers with electrodes : d_{31} and d_{33} piezoelectric layers

1.2.2. d_{33} - piezocomposites

For d_{33} piezocomposites, although the electric field lines do not have a constant direction (Figure 2b), when replacing the active layer by an equivalent homogeneous layer, we consider that the poling direction is that of the fibers (direction 3, Figure 3b), and that the electric field is in the same direction. With this reference frame, the plane stress hypothesis implies that $T_1 = 0$. The constitutive equations are given by

$$\begin{Bmatrix} T_2 \\ T_3 \\ T_4 \\ T_5 \\ T_6 \\ D_3 \end{Bmatrix} = \begin{bmatrix} c_{22}^{E*} & c_{23}^{E*} & 0 & 0 & 0 & -e_{32}^* \\ c_{32}^{E*} & c_{33}^{E*} & 0 & 0 & 0 & -e_{33}^* \\ 0 & 0 & c_{44}^{E*} & 0 & 0 & 0 \\ 0 & 0 & 0 & c_{55}^{E*} & 0 & 0 \\ 0 & 0 & 0 & 0 & c_{66}^{E*} & 0 \\ e_{32}^* & e_{33}^* & 0 & 0 & 0 & \varepsilon_{33}^{S*} \end{bmatrix} \begin{Bmatrix} S_2 \\ S_3 \\ S_4 \\ S_5 \\ S_6 \\ E_3 \end{Bmatrix} \tag{4}$$

For both types of piezocomposites, matrix $\left[c^{E*}\right]$ is a function of the longitudinal (in the direction of the fibers) and transverse in-plane Young's moduli (E_L and E_T), the in plane Poisson's ratio ν_{LT}, the in-plane shear modulus

G_{LT}, and the two out-of-plane shear moduli G_{Lz} and G_{Tz}. Matrix $[e^*]$ is given by

$$[e^*] = [d]\left[c^{E*}\right] \tag{5}$$

where

$$[d] = \left[\begin{array}{ccccc} d_{31} & d_{32} & 0 & 0 & 0 \end{array}\right] \tag{6}$$

in the case of d_{31} piezocomposites and

$$[d] = \left[\begin{array}{ccccc} d_{32} & d_{33} & 0 & 0 & 0 \end{array}\right] \tag{7}$$

in the case of d_{33} piezocomposites. Note that the coefficients d_{ij} are unchanged under the plane stress hypothesis.

2. Numerical evaluation of equivalent properties of piezocomposites

Homogenization techniques are widely used in composite materials. They consist in computing the homogeneous, equivalent properties of multi-phase heterogeneous materials. An example of a 1-3 composite is shown on Figure 4 (1-3 refers to the fact that the fibers are connected in one direction and the matrix in all 3 directions). The material is a periodic repetition in all three directions of a so-called representative volume element (RVE) also shown in the figure.

Equivalent properties are obtained by writing the constitutive equations (Equation (3) or (4) in this case) in terms of the average values of T_i, S_i, D_i, E_i on the RVE:

$$\begin{aligned} \overline{T_i} &= \frac{1}{V}\int_V T_i dV \qquad & \overline{D_i} &= \frac{1}{V}\int_V D_i dV \\ \overline{S_i} &= \frac{1}{V}\int_V S_i dV \qquad & \overline{E_i} &= \frac{1}{V}\int_V E_i dV \end{aligned} \tag{8}$$

where $\overline{\ }$ denotes the average value.

A tremendous amount of literature exists on homogenization of elastic and inelastic materials [11, 12, 13]. Extensions have also been made to elastic piezoelectric materials in [14, 15, 16, 17, 18, 19] where analytical results

have been developed. The difficulty with analytical approaches is that they are often restricted to particular geometries (circular or elliptical fibers) and do not take into account complicated electrode patterns such as interdigitated electrodes. The use of numerical approaches such as the finite element method allows to overcome this problem. The principle consists in meshing the RVE and computing approximations of the solution on this RVE using numerical techniques. To our knowledge, this technique has only been applied for **Active Fiber Composites (AFC)** actuated in the d_{33}-mode. In the model of the RVE, some simplifying assumptions are often made. The first one consists in applying a uniform electric field instead of the real curved electric field [20, 21]. The second one consists in considering that the poling direction is uniform and in the fiber direction [22]. Both these aspects have been taken into account recently in [23] for the evaluation of stress concentration in AFCs, but no homogenization was performed. In addition, the hypothesis that the faces of the RVE remain plane is also often made. The first problem related with this hypothesis is that it results in a large overestimation of the shear stiffness constants. The second problem is that it is not representative of the fact that these transducers are periodic only in two directions (in the plane of the actuator).

The method developed in this paper is inspired from [24] but, due to the specificities of MFC transducers, and the remarks formulated above, differs in the following points: (i) we consider periodicity only in the plane of the actuator, since the thickness of the rectangular fibers is of the same order of magnitude as the thickness of the transducer, (ii) the electrodes are modeled in the RVE (Figure 5), and the macro variable V representing the voltage difference across the electrodes is used instead of the electric field, resulting in additional electrical equipotential conditions, as well as curved electric field lines in the case of d_{33} MFCs, (iii) the poling direction is not necessarily aligned in the direction of the fibers, but follows the electric field lines imposed by the electrodes configuration. **Note that a MFC contains more than fifty fibers so that it can be considered as periodic in the direction perpendicular to the fibres.**

2.1. Finite element based periodic homogenization of MFCs

When used as sensors or actuators, piezocomposite transducers are typically equipped with two electrodes. These electrodes impose an equipotential

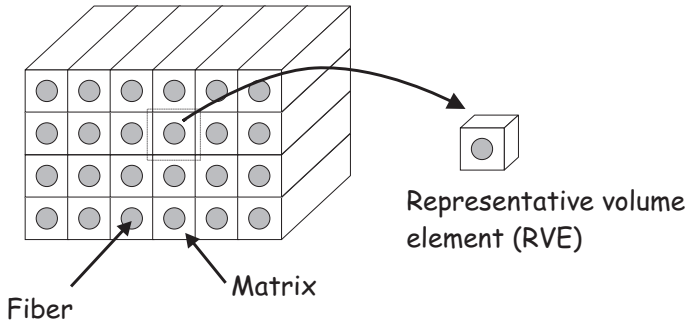

Figure 4: Example of a 1-3 composite and its representative volume element (RVE)

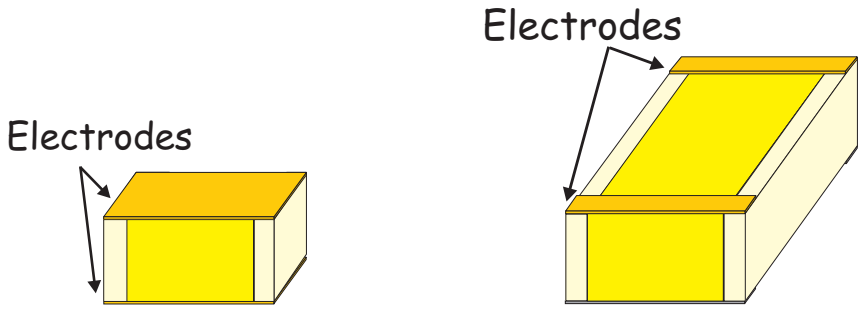

Figure 5: Representative volume element (RVE) for a d_{31} and a d_{33} MFC including the electrodes

voltage on their surfaces, and the electrical variables are the voltage difference V across the electrodes, and the electrical charge Q. These two variables are representative of the electrical macro variables which will be used in the numerical models of structures equipped with such transducers: transducers are used either in open-circuit conditions ($Q = 0$ or imposed) or short-circuit conditions ($V = 0$ or imposed). Instead of the average values of D_i and E_i, the macro variables Q and V are therefore used in the homogenization process. For a homogeneous d_{33} transducer (Figure 6), the constitutive equations can be rewritten in terms of these macro variables:

$$\begin{Bmatrix} T_2 \\ T_3 \\ T_4 \\ T_5 \\ T_6 \\ Q \end{Bmatrix} = \begin{bmatrix} c_{22}^{(SC*)} & c_{23}^{(SC*)} & 0 & 0 & 0 & -e_{32}^*/p \\ c_{32}^{(SC*)} & c_{33}^{(SC*)} & 0 & 0 & 0 & -e_{33}^*/p \\ 0 & 0 & c_{44}^{(SC*)} & 0 & 0 & 0 \\ 0 & 0 & 0 & c_{55}^{(SC*)} & 0 & 0 \\ 0 & 0 & 0 & 0 & c_{66}^{(SC)*} & 0 \\ e_{32}^*A & e_{33}^*A & 0 & 0 & 0 & \varepsilon_{33}^{s*}A/p \end{bmatrix} \begin{Bmatrix} S_2 \\ S_3 \\ S_4 \\ S_5 \\ S_6 \\ -V \end{Bmatrix} \tag{9}$$

where SC stands for 'short-circuit' ($V = 0$), p is the length of the transducer, A is the surface of the electrodes of the equivalent homogeneous transducer and Q is the charge collected on the electrodes.

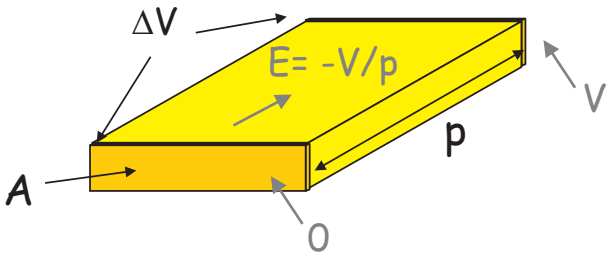

Figure 6: Homogeneous model of the d_{33} piezocomposite and definition of the macro variables

For d_{31}-piezocomposites, the approach is identical.

2.1.1. Definition of local problems

The RVE is made of two different materials. In order to find the homogeneous constitutive equations, Equation (9) is written in terms of the average values of the mechanical quantities S_i and T_i in the RVE and the electrical variables Q and V defined on the electrodes:

$$\begin{Bmatrix} \overline{T_2} \\ \overline{T_3} \\ \overline{T_4} \\ \overline{T_5} \\ \overline{T_6} \\ Q \end{Bmatrix} = \begin{bmatrix} \overline{c_{22}}^{(SC*)} & \overline{c_{23}}^{(SC*)} & 0 & 0 & 0 & -\overline{e_{32}}^{*}/p \\ \overline{c_{32}}^{(SC*)} & \overline{c_{33}}^{(SC*)} & 0 & 0 & 0 & -\overline{e_{33}}^{*}/p \\ 0 & 0 & \overline{c_{44}}^{(SC*)} & 0 & 0 & 0 \\ 0 & 0 & 0 & \overline{c_{55}}^{(SC*)} & 0 & 0 \\ 0 & 0 & 0 & 0 & \overline{c_{66}}^{(SC*)} & 0 \\ \overline{e_{32}}^{*}A & \overline{e_{33}}^{*}A & 0 & 0 & 0 & \overline{\varepsilon_{33}}^{S*}A/p \end{bmatrix} \begin{Bmatrix} \overline{S_2} \\ \overline{S_3} \\ \overline{S_4} \\ \overline{S_5} \\ \overline{S_6} \\ -V \end{Bmatrix} \tag{10}$$

The different terms in Equation (10) can be identified by defining local problems on the RVE. The technique consists in imposing conditions on the different strain components and V and computing the average values of the stress and the charge in order to find the different coefficients. For the electric potential, two different conditions ($V = 0, 1$) are used. For the mechanical part, we assume that the displacement field is periodic in the plane of the transducer (see i.e [24]): on the boundary of the RVE (but not on the upper and lower surfaces since the piezocomposite is not periodic in that direction), the displacement can be written:

$$u_i = \overline{S}_{ij}\, x_j + v_i \tag{11}$$

where u_i is the i^{th} component of displacement, $\overline{S}_{ij}$ is the average strain in the RVE (tensorial notations are used), x_j is the j^{th} spatial coordinate of the point considered on the boundary, and v_i is the periodic fluctuation on the RVE. The fluctuation v is periodic in the plane of the transducer so that between two opposite faces (noted B^-/B^+ and C^-/C^+, Figure 7), one can write ($v(x_j^{K+}) = v(x_j^{K-})$, $K = B, C$):

$$u_i^{K+} - u_i^{K-} = \overline{S}_{ij}\,(x_j^{K+} - x_j^{K-}) \qquad K = B, C \tag{12}$$

For a given value of the average strain tensor ($\overline{S}_{ij}$), Equation (12) defines constraints between the points on each pair of opposite faces. This is illustrated in Figure 8, where an average strain S_2 is imposed on the RVE and the constraints are represented for u_2 on faces B^- and B^+.

Note that these constraints do not impose that the faces of the RVE remain plane, which is important for the evaluation of the shear stiffness coefficients. For faces A^- and A^+, the displacement is unconstrained in the normal direction, because the MFC is not periodic in this direction.

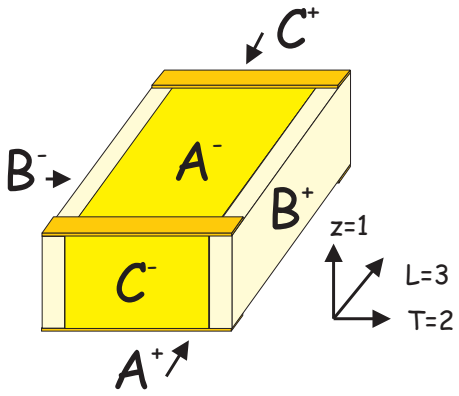

Figure 7: Definition of pairs of opposite faces on the RVE

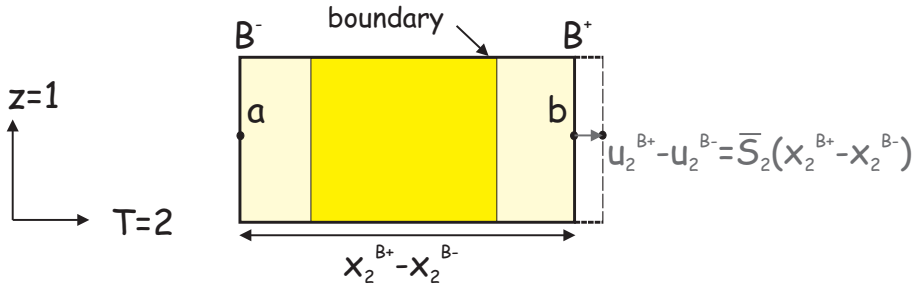

Figure 8: Example of an average strain S_2 imposed on the RVE and associated periodic conditions

In total, six local problems are needed to identify all the coefficients in (10) (Figure 9). The first problem consists in applying a difference of potential V to the electrodes of the RVE and imposing zero displacement on all the faces (except the top and bottom). The deformed mesh resulting from the finite element computation for this local problem is represented in Figure 10 for a d_{31}-MFC. In the next five local problems, the difference of potential is set to 0 (short-circuited condition), and five deformation mechanisms are induced. Each of the deformation mechanisms consists in a unitary strain in one of the directions (with zero strain in all the other directions). For each case, the average values of T_i and S_i, and the charge accumulated on the electrodes Q, are computed, and used to determine all the coefficients in (10), from which the engineering constants are determined. **Note that the electrodes are included in a particular layer which is in direct contact with the active layer considered for homogenization, so that they are modeled as an electrical boundary condition on the RVE only. The mechanical properties of the electrodes should be taken into account when modeling the full MFC, as detailed in [10].**

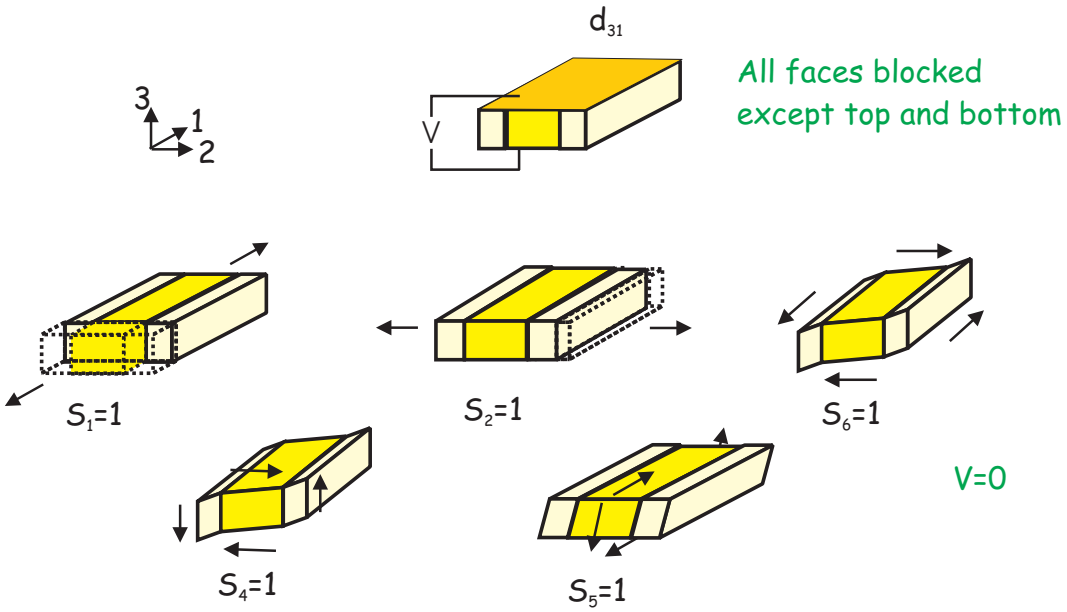

Figure 9: The six local problems solved by the finite element method in order to compute the homogenized properties of d_{31}-MFCs

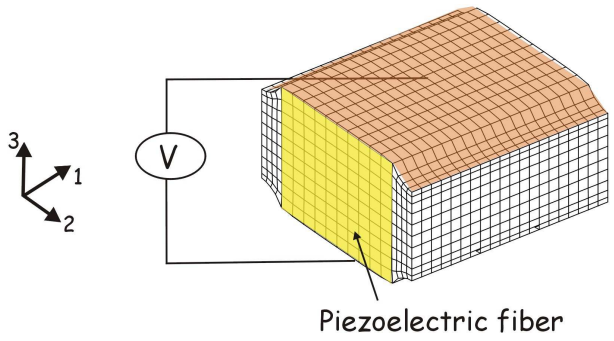

Figure 10: Deformation of the RVE of a d_{31}-MFC under applied electric potential difference V between the top and bottom electrodes computed using finite element 3D piezoelectric elements. All faces are fixed except top and bottom (fiber volume fraction $\rho = 0.9$).

2.2. Comparison with the analytical mixing rules

2.2.1. d_{31} MFCs

The homogeneous properties of d_{31}-MFCs have been computed for different volume fractions between $\rho = 0$ and $\rho = 1$ (bulk ceramic) using the mixing rules developed in [10] and the numerical method presented in section 2.1. **A comparison with experimental results would also be very useful but MFC properties have only been measured for a single volume fraction of fibers ($\rho = 0.86$). A comparison with these measurements can be found in [10].**

The properties of the fibers are given in Table 1 (it is assumed that the fibers are made of SONOX P502 from $CeramTec$, direction 3 is the poling direction. For more details, see [25]). For the matrix, typical values for epoxy are considered: $E = 2.9GPa$, $\nu = 0.3$ and $\varepsilon_{11}^T/\varepsilon_0 = \varepsilon_{22}^T/\varepsilon_0 = \varepsilon_{33}^T/\varepsilon_0 = 4.25$.

The evolution of the different mechanical, piezoelectric and dielectric properties as a function of the fiber volume fraction is represented on Figures 11 and 12. Direction L corresponds to the fiber direction, T is the transverse direction, and z is the out-of-plane direction.

For the mechanical properties, the match is very good for E_L, E_T, G_{LT} and ν_{LT}. For G_{Lz} and G_{Tz}, the numerical results are higher, especially for high volume fractions of fibers. This is due to the presence of an inhomogeneous electric field in the Lz plane, mainly in the L direction for G_{Lz}, and in

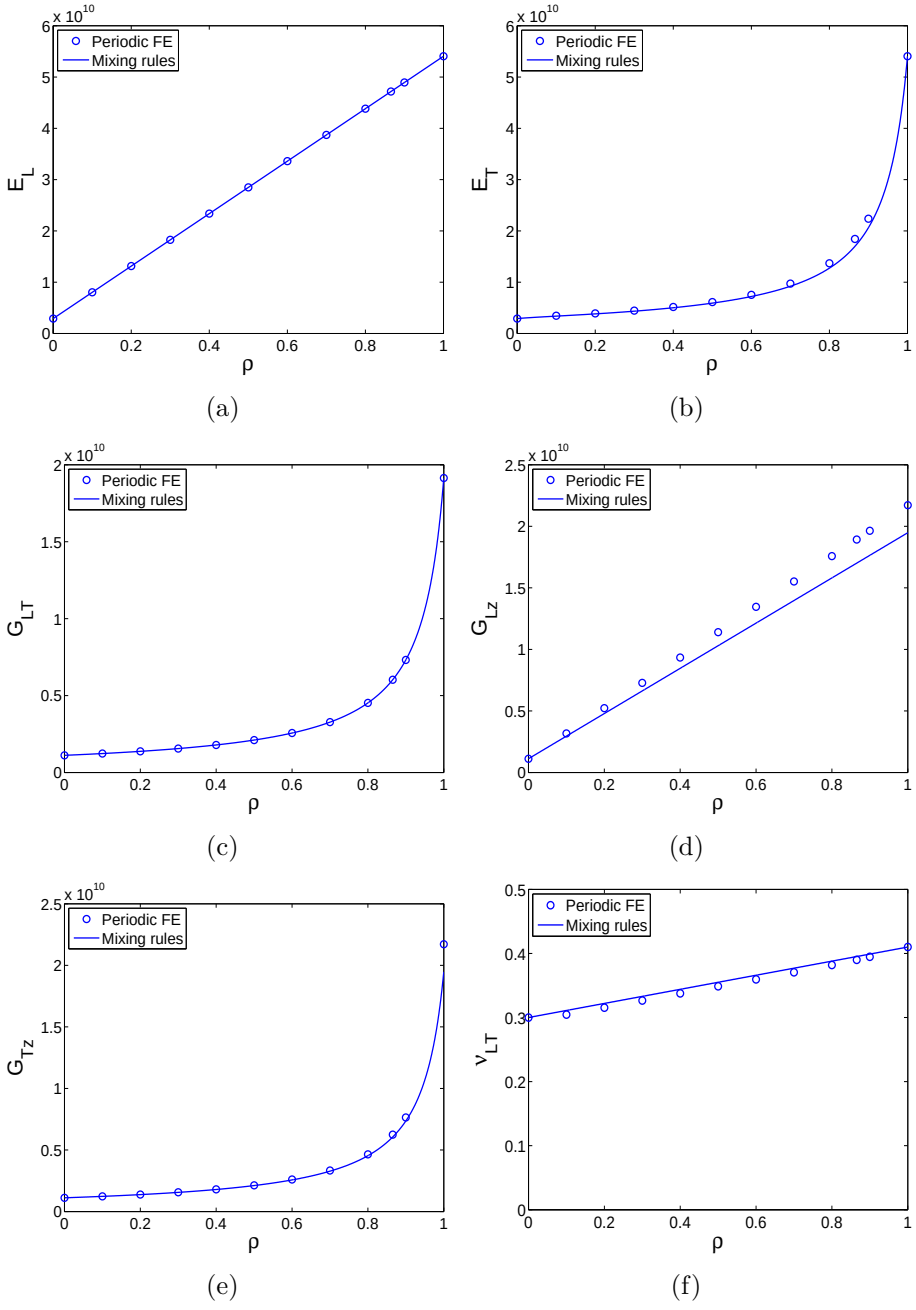

Figure 11: Evolution of the mechanical properties of d_{31} MFCs as a function of the fiber volume fraction: comparison between the mixing rules and periodic finite element homogenization

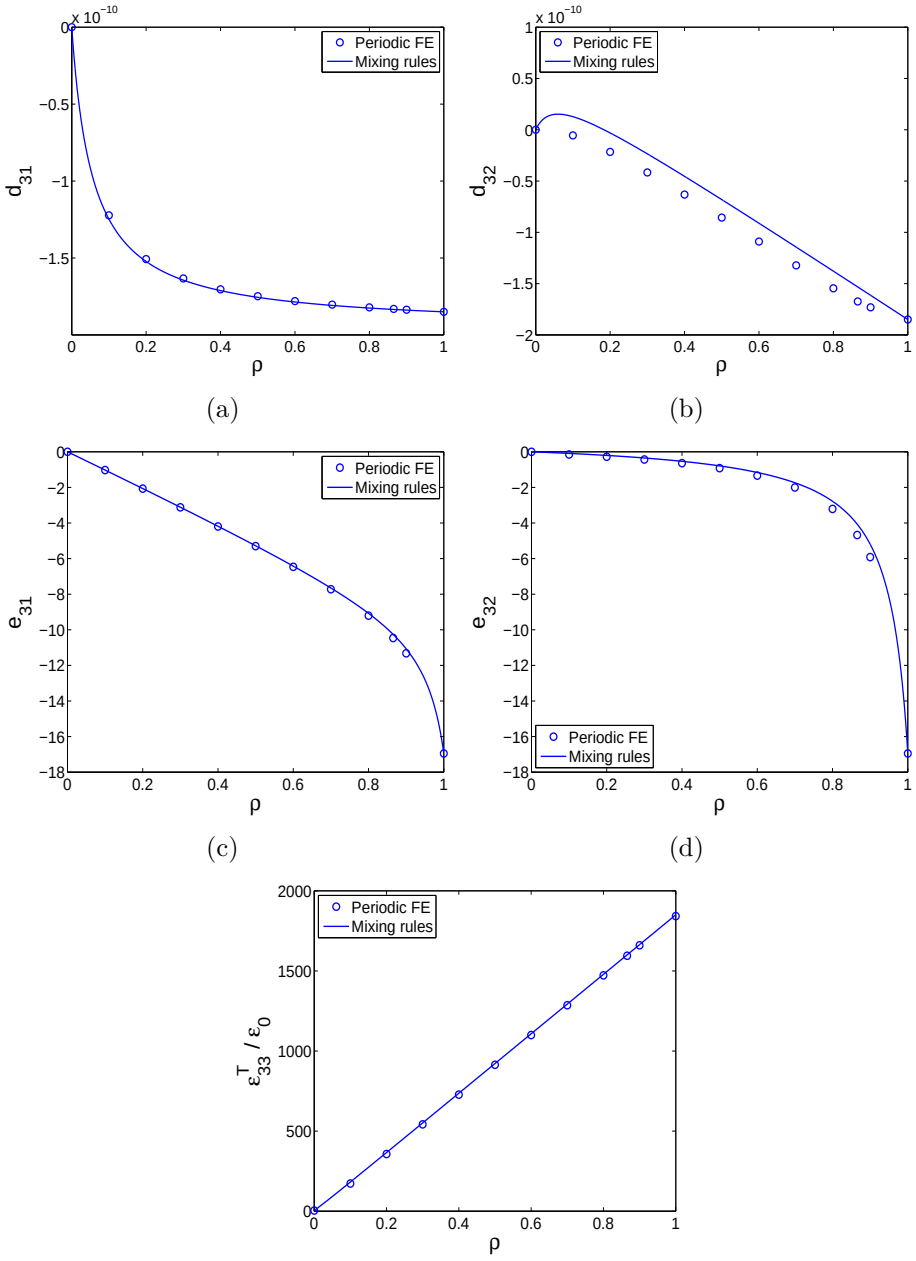

Figure 12: Evolution of piezoelectric and dielectric properties of d_{31} MFCs as a function of the fiber volume fraction: comparison between the mixing rules and periodic finite element homogenization

MFC Fiber Engineering constants	Symbol	Unit	SONOX P502 (set 1)
Young's modulus	$E_1 = E_2$	GPa	54.05
	E_3	GPa	48.30
Shear modulus	$G_{23} = G_{31}$	GPa	19.48
	G_{12}	GPa	19.14
Poisson's ratio	$\nu_{23} = \nu_{13}$	-	0.44
	ν_{12}	-	0.41
Piezoelectric charge constants	$d_{32} = d_{31}$	pC/N	-185
	d_{33}	pC/N	440
	$d_{15} = d_{24}$	pC/N	560
Dieletric relative constants (free)	$\varepsilon_{11}^T/\varepsilon_0 = \varepsilon_{22}^T/\varepsilon_0$	-	1950
	$\varepsilon_{33}^T/\varepsilon_0$	-	1850

Table 1: MFC fibers engineering constants

the Tz plane, mainly in the T direction for G_{Tz} (Figure 13). If zero electric potential was imposed on all the faces of the RVE instead of the real short-circuit conditions (this is done for example in [24, 20, 21]), these electric fields would not be present and there would be no stiffening of the piezocomposite for high volume fractions. This corresponds to the hypothesis made in the uniform field method (UFM) used to derive the mixing rules. Imposing zero potential on the actual electrodes only, leads therefore to interesting results different from the ones traditionally found in the literature.

For the piezoelectric properties, the match is very good for d_{31}, and good for d_{32} despite of a larger discrepancy for low volume fractions. Note however that the match is good for e_{31} and e_{32} which are most often used in shell finite element formulations. The difference between the mixing rules and the numerical approach is due to the inhomogeneity of the different fields in the finite element approach. It has been found that this inhomogeneity comes mainly from the plane stress assumption which results in deformed shapes of the kind reported in Figure 14, where one sees that the out-of-plane stresses and strains are not uniform in the fiber and the matrix. Note that this analysis is different from the one presented in [25] where the fields were much more uniform because the periodicity conditions was imposed in

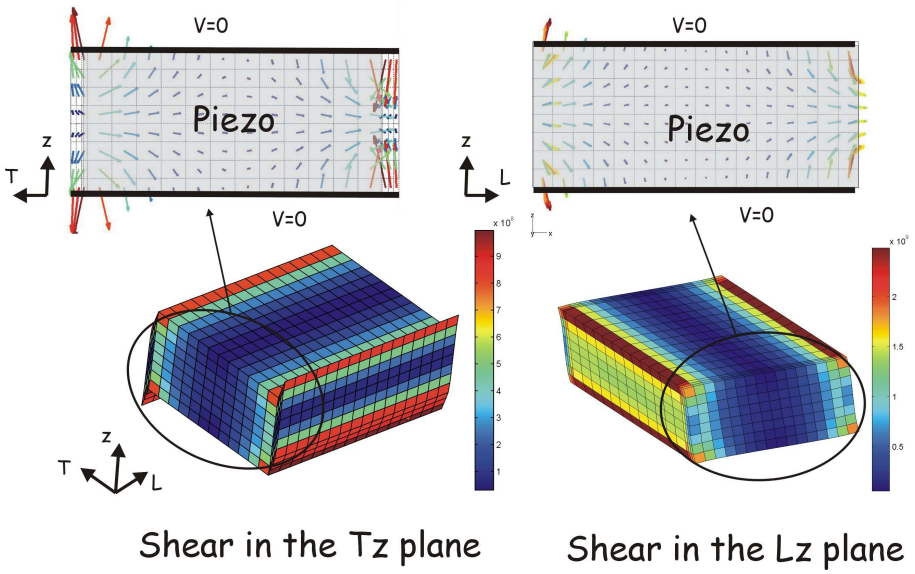

Figure 13: Electric fields in the piezocomposite due to a shear strain in short-circuited conditions. RVE with $\rho = 0.9$

the direction perpendicular to the plane of the actuator.

2.2.2. d_{33} MFCs

The RVE used for the periodic finite element homogenization is shown in Figure 15. It includes the definition of the interdigitated electrodes. The length of the RVE (p), corresponding to the distance between the finger electrodes, is 6 times the thickness h of the transducer (for a study of the influence of this ratio, see [1]) and the width of the electrodes is equal to this thickness. In a first study, it is assumed that the poling direction is parallel to the fiber direction. This hypothesis will be further discussed in section 2.2.3.

The evolution of the different mechanical, piezoelectric and dielectric properties as a function of the fiber volume fraction is represented in Figures 16 and 17 where they are compared with the analytical mixing rules.

For the mechanical properties, the match is good, but there is a stiffening for the longitudinal modulus and the two shear moduli G_{Lz} and G_{Tz} for high volume fractions of PZT. This is due to the presence of an electric field in

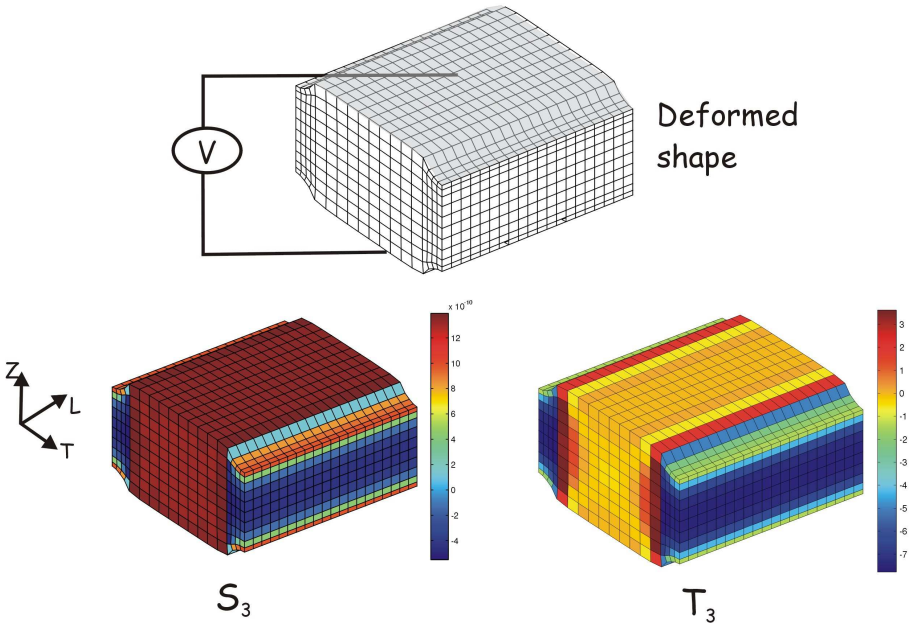

Figure 14: Deformed shaped under the plane stress assumption when an electric potential diffierence is applied to the electrodes. The out-of-plane stresses and strains are not uniform. RVE with $\rho = 0.9$

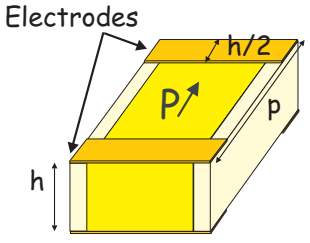

Figure 15: Representative volume element (RVE), p/h=6

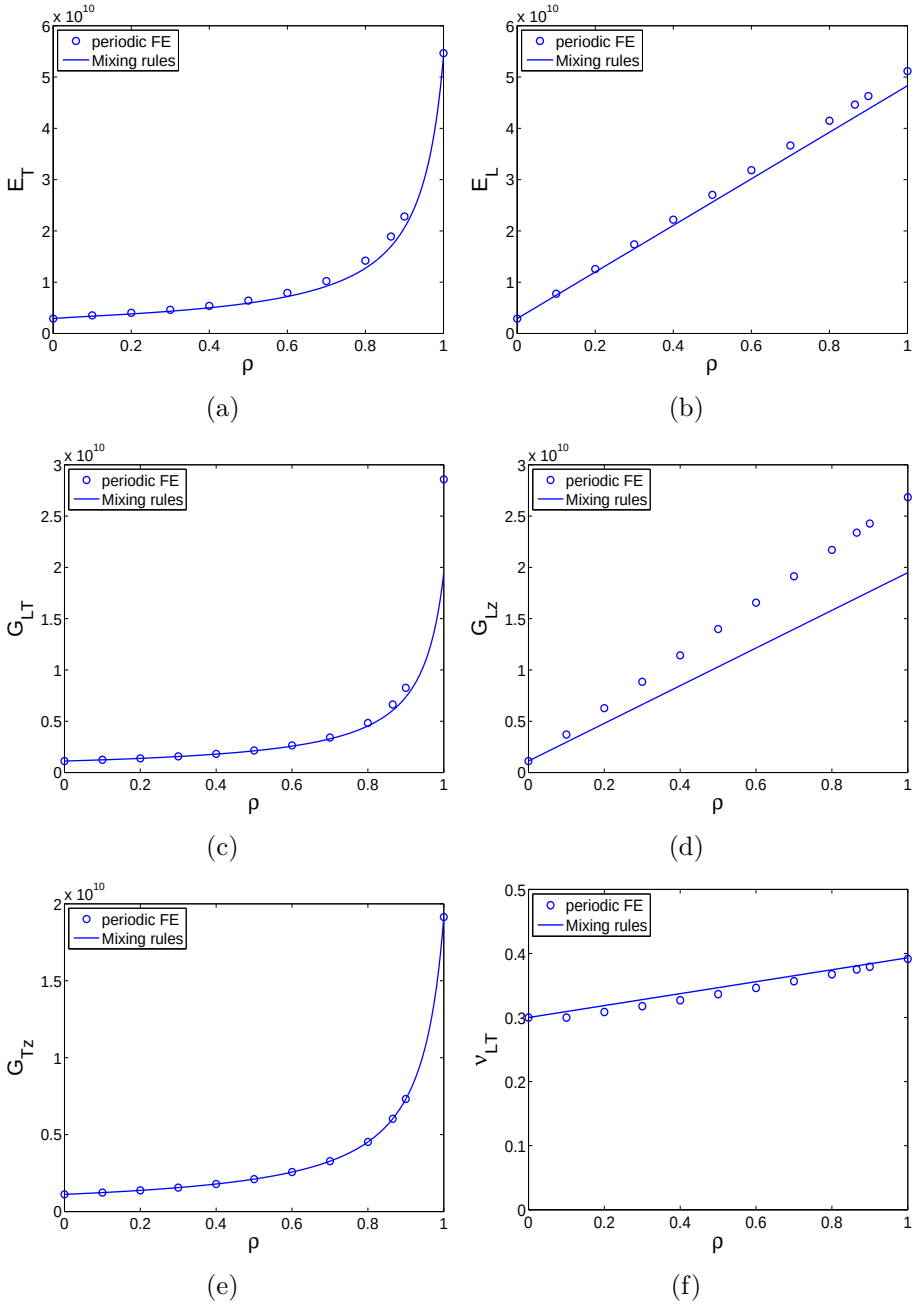

Figure 16: Evolution of the mechanical properties of d_{33} MFCs as a function of the fiber volume fraction: comparison between the mixing rules and periodic finite element homogenization

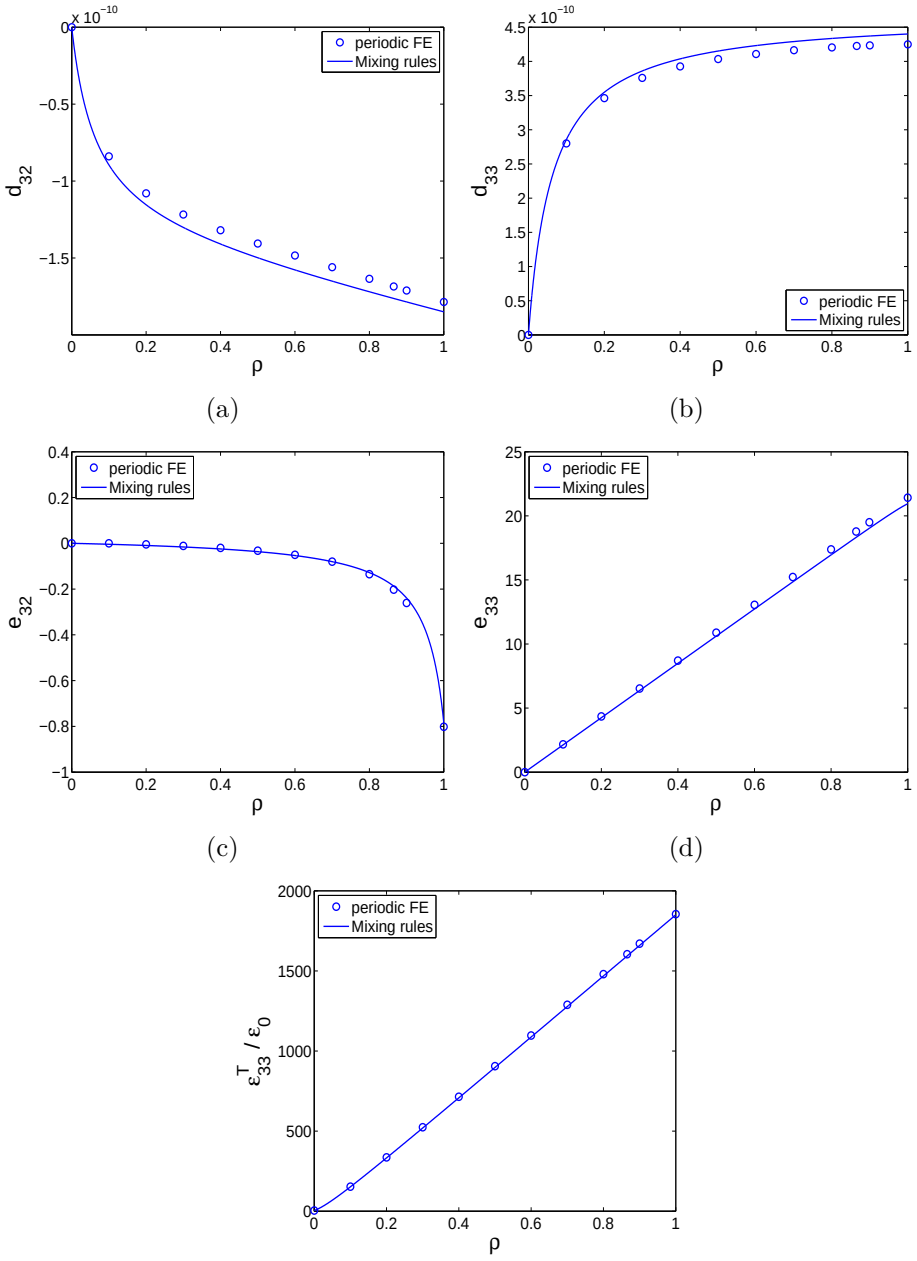

Figure 17: Evolution of piezoelectric and dielectric properties of d_{33} MFCs as a function of the fiber volume fraction: comparison between the mixing rules and periodic finite element homogenization

the composite in short-circuited conditions (Figure 18, similar to what was observed for d_{31}-MFCs). It is interesting to note that for the shear moduli, the stiffening is stronger than in the case of d_{31}-MFCs. This is due to the fact that the electrode is not continuous on the top and bottom faces, so that a stronger and more homogeneous electric field can develop in the region between the electrodes. For the longitudinal modulus, the appearance of the electric field is due to the existence of curved electric field lines.

For the piezoelectric properties, the match is good for e_{31} and e_{32}. The values of d_{32} and d_{33} are slightly lower than the values computed using the mixing rules. This effect is directly related to the stiffening of the piezocomposite in the longitudinal direction due to the presence of electric fields in short-circuited conditions.

Another interesting remark is that the free strain is not uniform (Figure 19). In the region below the electrodes, the electric field is not aligned with the poling direction and changes direction and magnitude quickly. The average induced stress is however equivalent to an ideal d_{33} actuator for which $E_3 = -V/p$. This is because the value of the electric field in the region between the electrodes has been found to be approximately equal to $E_3 = -V/(p-h)$ so that it is stronger than for the ideal d_{33} (for which $E_3 = -V/p$) and compensates for the inactive zone below the electrodes.

2.2.3. Influence of the poling direction for d_{33} MFCs

Figure 20 shows the amplitude and direction of the electric field for a d_{33}-MFC ($\rho = 0.9$) resulting from the application of a potential difference on the interdigitated electrodes. During the manufacturing, the poling of the piezoelectric fibers is done by imposing very high electric fields to the interdigitated electrodes. This results in a poling direction aligned with the applied electric field. The hypothesis that the poling direction is in the fiber direction is therefore only valid in the region between the finger electrodes.

In order to take this into account, we have corrected the finite element computations by introducing a local polarization vector in each element which is aligned with the electric field. In a first step, the electric field lines are computed with the poling vector aligned with the fiber direction L. In a second step, the poling direction is adjusted and aligned with the electric field lines as shown in Figure 20. In Figures 21 and 22, we compare

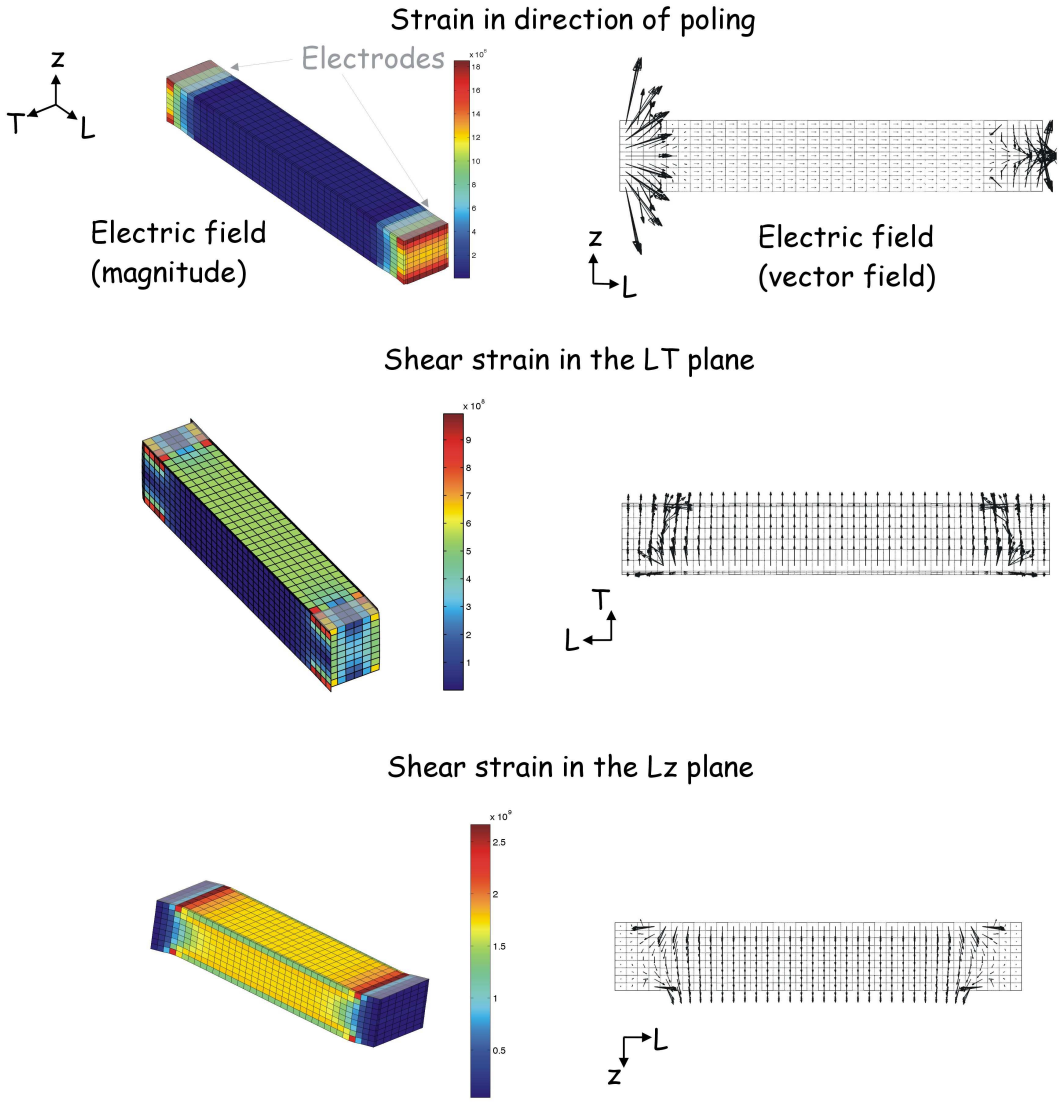

Figure 18: Electric fields in the piezocomposite due to a longitudinal strain and shear strains in short-circuited conditions. RVE with $\rho = 0.9$

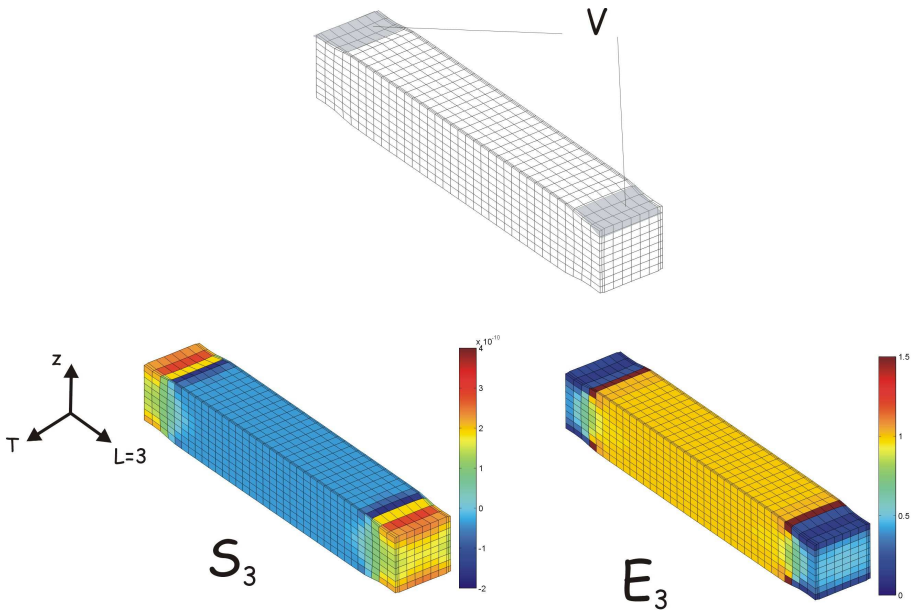

Figure 19: Induced strain S_3 and electric field E_3 due to the application of a potential difference V. RVE with $\rho = 0.9$

the results obtained with the polarization in the direction of the fibers and the polarization aligned with the electric field. The figures show that there is a minor difference due to a stronger stiffening in the longitudinal direction. This is due to an increase in non-zero electric field between the short circuited electrodes when the polarization is aligned with the electric field.

The direction of poling has a small influence on the average behavior of the d_{33} piezocomposite because the regions below the electrodes do not contribute very much to the overall behavior. If one is concerned with more local values such as stress concentrations which occur in the regions below the electrodes, this influence may be important and should be further studied [23].

3. Conclusion

In this paper, finite element periodic homogenization has been applied to both d_{31} and d_{33} MFC transducers. The method presented differs from the ones traditionally found in the literature in three main aspects: (i) periodicity

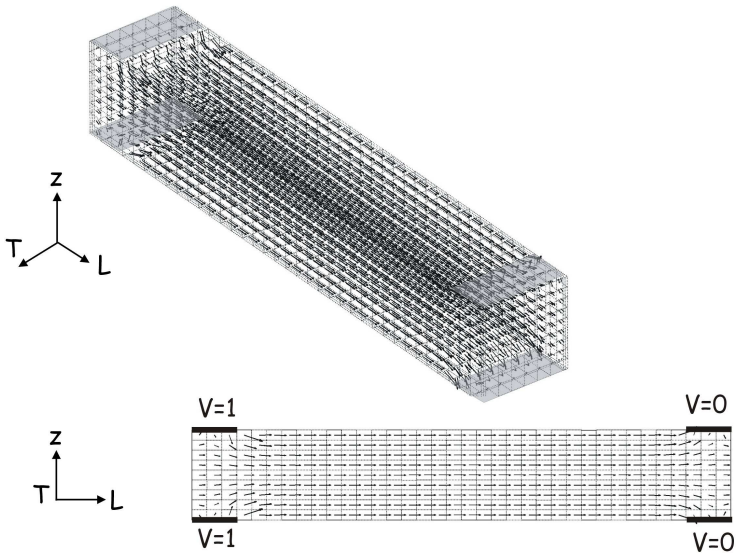

Figure 20: Electric field (direction and amplitude) due to the application of an electrical potential difference V. RVE with $\rho = 0.9$

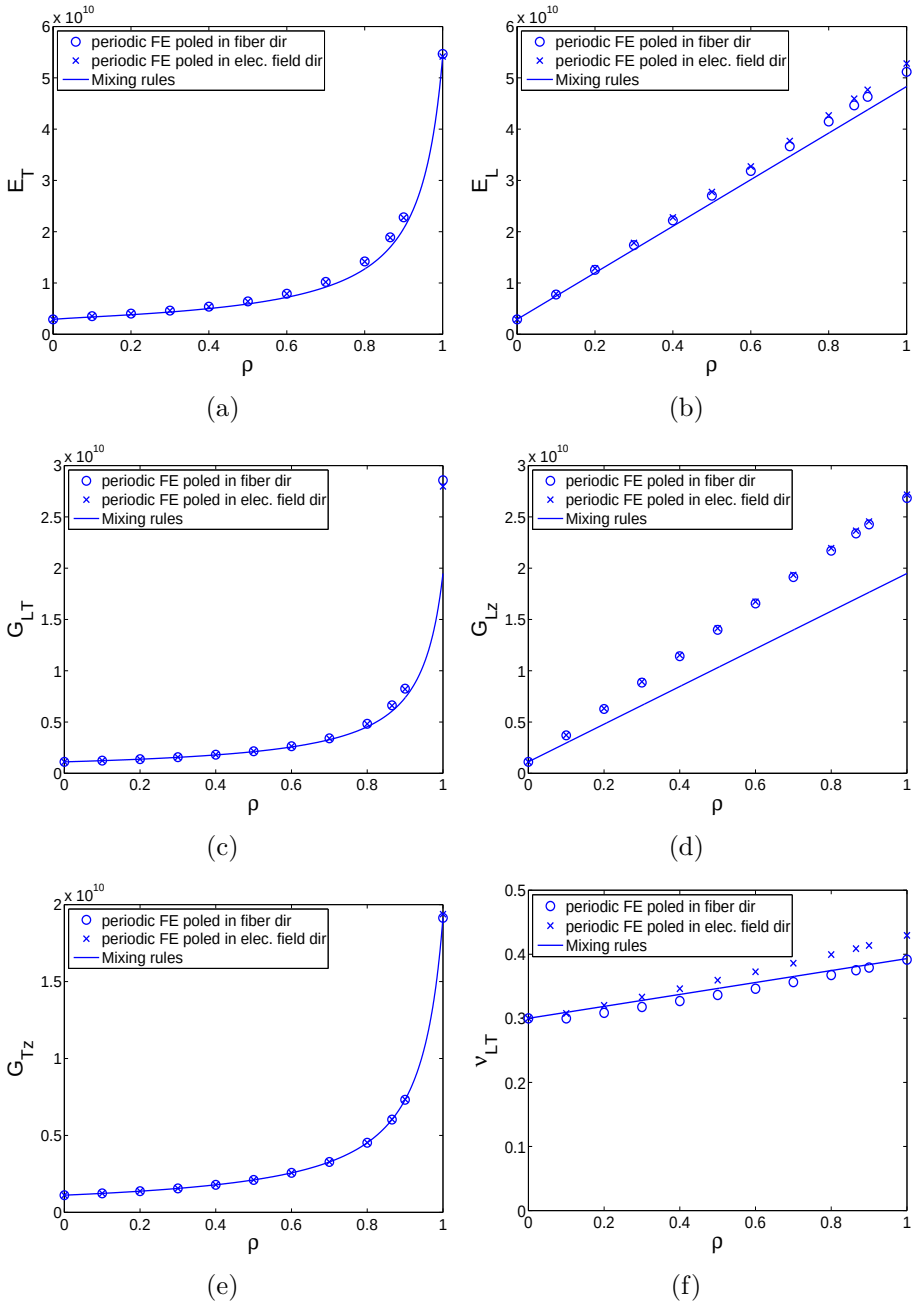

Figure 21: Evolution of the mechanical properties of d_{33} MFCs as a function of the fiber volume fraction: comparison between the mixing rules and periodic finite element homogenization (fibers poled in direction L or aligned with the electric field)

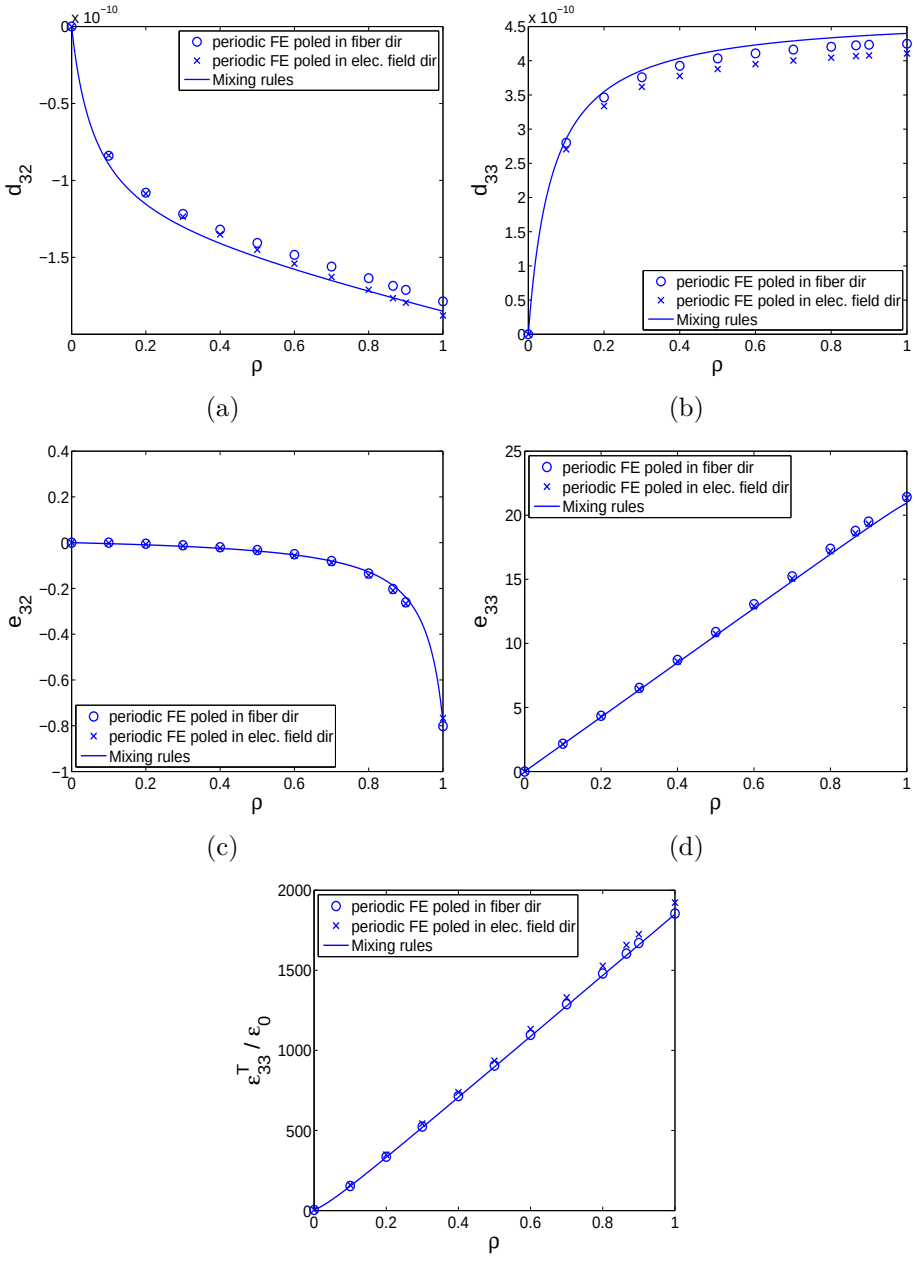

Figure 22: Evolution of piezoelectric and dielectric properties of d_{33} MFCs as a function of the fiber volume fraction: comparison between the mixing rules and periodic finite element homogenization (fibers poled in direction L or aligned with the electric field)

is enforced only in the plane of the transducer and not in all three directions, which is more representative of the fact that only one fiber is present through the thickness, (ii) the electrodes are modeled in the RVE, and the macro variables V and Q representing the voltage difference across the electrodes and the charge collected on the electrodes is used instead of the electric field, resulting in additional electrical equipotential conditions, as well as curved electric field lines in the case of d_{33} MFCs, (iii) the poling direction is not necessarily aligned in the direction of the fibers, but follows the electric field lines imposed by the electrodes configuration. The homogeneous properties of both d_{31} and d_{33} MFCs have been computed using this method for different volume fractions of fibers, and compared to previously published analytical mixing rules. Although there is in general a good agreement between the numerical and the analytical results, some differences were found due to: (i) the electrical boundary conditions and the curved electric field lines (in the case of d_{33}-MFCs) imposed by the specific electrodes configuration which are not taken into account in the analytical approach, and (ii) the non uniformity of the stress and strain fields resulting from the release of the periodicity condition in the perpendicular direction. This highlights the importance of correctly modeling the electrodes and performing the homogenization using the macro electrical variables V and Q rather than the local electric fields and electric displacements. For d_{33} MFCs, the influence of the poling direction, either aligned in the fiber direction, or aligned with the electric field lines (which corresponds to the reality for these types of transducers) has been studied. It has been shown that the influence on the homogenized properties was minor, although the influence on some local values (stress concentrations) can be high. The method presented is general and could be applied to other types of piezocomposites than the Macro Fiber Composites treated in this paper.

Acknowledgements

This work was supported in part by the Fond National de la Recherche Luxembourg in the context of the FNR MAFICOMECH Project (C08/MS/17).

References

[1] N. Hagood, R. Kindel, K. Ghandi, P. Gaudenzi, Improving transverse actuation of piezoceramics using interdigitated surface electrodes, in: N. W. Hagood (Ed.), Proc. SPIE Vol. 1917, 1993, pp. 341–352.

[2] K. Lazarus, M. Lundstrom, J. Moore, E. Crawley, Packaged strain actuator, US Patent 5687462.

[3] G. Horner, Piezoelectric composite device and method for making same, International patent application WO0217407.

[4] P. Wierach, Elektromechanisches funktionsmodul, German Patent DE 10051784 C1.

[5] W. Wilkie, R. Bryant, J. High, R. Fox, R. Hellbaum, A. Jalink, B. Little, P. Mirick, Low-cost piezocomposite actuator for structural control applications, in: Proc. SPIE 7th Annual Int. Symp. Smart. Struct. Mater., Newport Beach, USA, 2000.

[6] A. Bent, N. Hagood, J. Rodgers, Anisotropic actuation with piezoelectric fiber composites, J. Intell. Mater. Syst. Struct 6 (1995) 338–349.

[7] P. Wierach, Low profile piezo actuators based on multilayer technology, in: Proc. of 17th Int. Conf. on Adaptive Structures and Technologies (ICAST2006), Taipei, Taiwan, 2006.

[8] B. Williams, G. Park, D. Inman, W. Wilkie, An overview of composite actuators with piezoceramic fibers, in: Proc. of 20th Int. Modal Analysis Conference (IMAC), Los Angeles, USA, 2002.

[9] V. Piefort, Finite element modelling of piezoelectric active structures, Ph.D. thesis, Université Libre de Bruxelles (June 2001).

[10] A. Deraemaeker, H. Nasser, A. Benjeddou, A. Preumont, Mixing rules for the piezoelectric properties of Macro Fiber Composites, J. Intell. Mater. Syst. Struct 20(12) (2009) 1391–1518.

[11] Z. Hashin, S. Shtrikman, On some variational principles in anisotropic and nonhomogeneous elasticity, J. Mech. Phys. Solids 10 (1962) 335–342.

[12] Z. Hashin, S. Shtrikman, A variational approach to the theory of the elastic behaviour of multiphase materials, J. Mech. Phys. Solids 11 (1963) 127–140.

[13] Z. Xia, Y. Zhang, F. Ellyin, A unified periodical boundary conditions for representative volume elements of composites and applications, International Journal of Solids and Structures 40 (2003) 1907–1921.

[14] D. Skinner, R. Newnham, L. Cross, Flexible composite transducers, Mat. Res. Bull. 13 (1978) 599–607.

[15] R. Newnham, D. Skinner, L. Cross, Connectivity and piezoelectric-pyroelectric composites, Mat. Res. Bull. 13 (1978) 525–536.

[16] F. Levassort, M. Lethiecq, D. Certon, F. Patat, A matrix method for modeling electroelastic moduli of 0-3 piezo-composites, IEEE Transactions on Ultrasonics, Ferroelectrics, and Frequency Control 44(2) (1997) 445–452.

[17] M. Dunn, M. Taya, Micromechanics predictions of the effective electroelastic moduli of piezoelectric composites, Int. J. Solids Structures 30(2) (1993) 161–175.

[18] A. Agbossou, C. Richard, Y. Vigier, Segmented piezoelectric fiber composite for vibration control: fabricating and modeling of electromechanical properties, Composites Science and Technology 63 (2003) 871–881.

[19] J. Smay, J. Cesarano, A. Tuttle, J. Lewis, Piezoelectric properties of 3-X periodic Pb(ZrxTi1-x)O3 - polymer composites, Journal of applied physics 92(10) (2002) 6119–6127.

[20] C. Poizat, M. Sester, Effective properties of composites with embedded piezoelectric fibres, Computational Materials Science 16 (1999) 89–97.

[21] E. Lenglet, A. Hladky-Hennion, J. Debus, Numerical homogenization techniques applied to piezoelectric composites, J. Acoust. Soc. Am. 113 (2003) 826–833.

[22] A. Bent, N. Hagood, Piezoelectric fiber composites with interdigitated electrode, J. Intell. Mater. Syst. Struct 8 (1997) 903–919.

[23] R. Paradies, M. Melnykowycz, Numerical stress investigation for piezoelectric elements with a circular cross section and interdigitated electrodes, J. Intell. Mater. Syst. Struct 18 (2007) 963–972.

[24] H. Berger, S. Kari, U. Gabbert, R. Rodriguez-Ramos, J. Bravo-Castillero, R. Guinovart-Diaz, F. J. Sabina, G. A. Maugin, Unit cell models of piezoelectric fiber composites for numerical and analytical calculation of effective properties, Smart Mater. Struct. 15 (2006) 451–458.

[25] A. Deraemaeker, S. Benelechi, A. Benjeddou, A. Preumont, Analytical and numerical computation of homogenized properties of MFCs: Application to a composite boom with MFC actuators and sensors, in: Proc. III ECCOMAS thematic conference on Smart Structures and Materials, Gdansk, Poland, 2007.

Numerical evaluation of the equivalent properties of Macro Fiber Composite (MFC) transducers using periodic homogenization

Arnaud Deraemaeker[a], Houssein Nasser[b]

[a] *Université Libre de Bruxelles - BATir, 50 av F.D. Roosevelt, CP 194/02, B-1050 Brussels*
[b] *CRP Henri Tudor, 29 Avenue John F. Kennedy, L-1855 Luxembourg*

Abstract

This paper focuses on the evaluation of the homogeneous properties of the active layer in Macro Fiber Composite (MFC) transducers using finite element periodic homogenization. The proposed method is applied to both d_{31} and d_{33} MFCs and the results are compared to previously published analytical mixing rules, showing a good agreement. The main advantages of the finite element homogenization is the possibility to take into account local details in the representative volume element such as complicated electrode patterns or local variations of the poling direction due to curved electric field lines. Although these influences have been found to be rather small in the present study, the method presented is useful for a better understanding of the behavior of piezocomposite transducers.

Keywords: Piezoelectric material, piezocomposite transducer, Macro Fiber Composite (MFC), Periodic homogenization, finite element method

1. Introduction

1.1. Piezocomposite transducers

Thin piezoelectric actuators and sensors are used in a variety of applications such as active vibration control, structural health monitoring or shape control. In these applications, PZT ceramics are commonly used due to their relatively low cost, high bandwidth and good actuation capabilities. The major drawbacks of these ceramics are their brittleness and very low flexibility. This problem can be overcome using piezocomposite transducers in which

piezoelectric fibers are mixed with a softer passive epoxy matrix. A typical piezocomposite transducer is made of an active layer sandwiched between two soft thin encapsulating layers (Figure 1). The packaging plays two different roles: (i) applying prestress to the active layer in order to avoid cracks, and (ii) bringing the electric field to the active layer through the use of a specific surface electrode pattern. The electrodes can be either continuous, in which case a voltage difference is applied between the top and bottom electrodes resulting in an electric field perpendicular to the plane of the transducer, or interdigitated [1], resulting in a curved electric field mostly aligned in the direction of the fibers (Figure 2). In the first case, the piezoelectric fibers are driven in the d_{31} mode, while in the second case, the fibers are driven in the d_{33}-mode, resulting in a higher achievable free strain but for much higher applied voltages. In the family of piezocomposite transducers, there exist many different types, differing mainly in the electrode configuration and the type of active layer which can consist of a bulk ceramic [2, 3, 4], large square [5] or round fibers [6], or even small fibers (see for example [7] and [8] for a review of these different types of piezocomposites).

Round fibers are usually not very effective due to the problem of dielectric permittivity mismatch which forces the electrodes to be in direct contact with the active fibers. For this reason and also for reasons linked to the manufacturing, the most successful implementation of piezocomposite transducers is probably the Macro Fiber Composites (MFC) manufactured and sold by the company *Smart Material*. Both d_{31} and d_{33} actuators and sensors have been developed and are currently sold.

In general, for a correct design of active vibration control or structural health monitoring systems, it is useful to develop numerical models (i.e. finite element models) of the structure equipped with piezoelectric transducers. For thin plate-like structures, three-dimensional volume finite elements should be avoided and an adequate approach is the use of multi-layer shell elements including piezoelectric layers [9]. Such elements are available in commercial finite element softwares such as SAMCEF (http://www.samcef.com) or the *Structural Dynamics Toolbox (SDT)* (http://www.sdtools.com) under *Matlab*. In this approach, the active layer is not modeled in details, but by an homogeneous active layer for which the equivalent properties need to be known. Unfortunately, the information found in the datasheet is not sufficient to determine all the mechanical, dielectric and piezoelectric equivalent

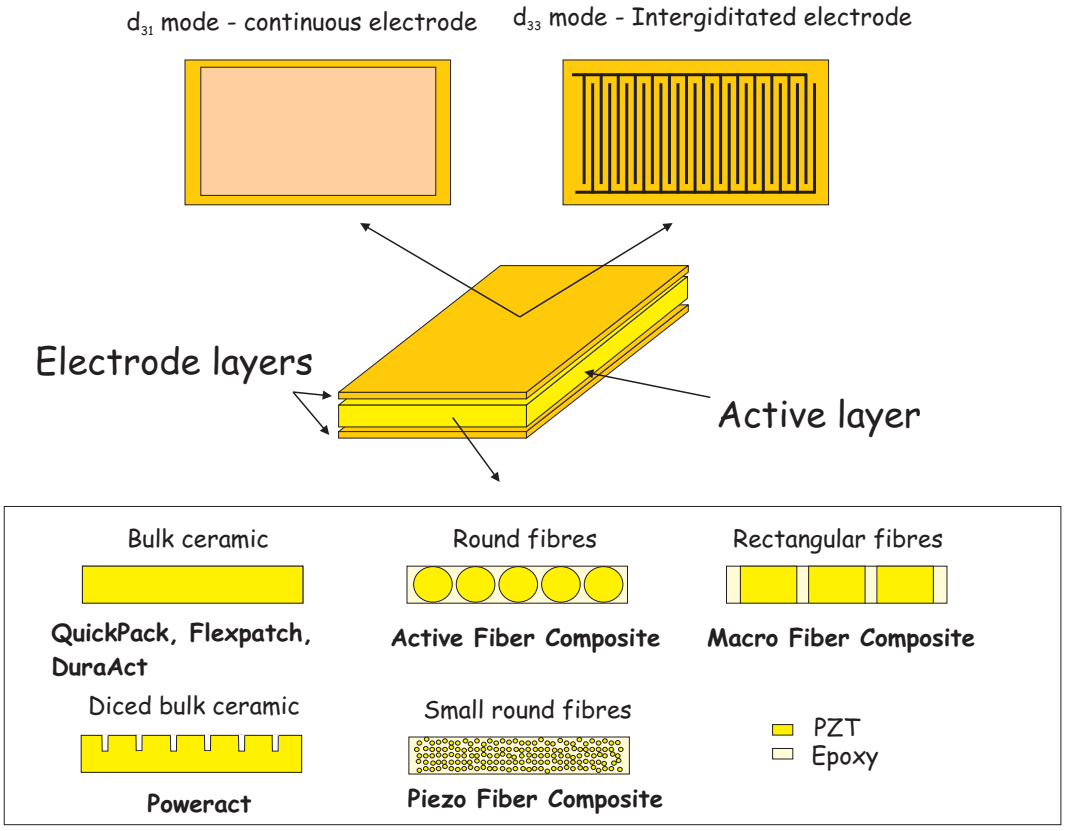

Figure 1: Overview of flat piezocomposite transducers with surface electrodes

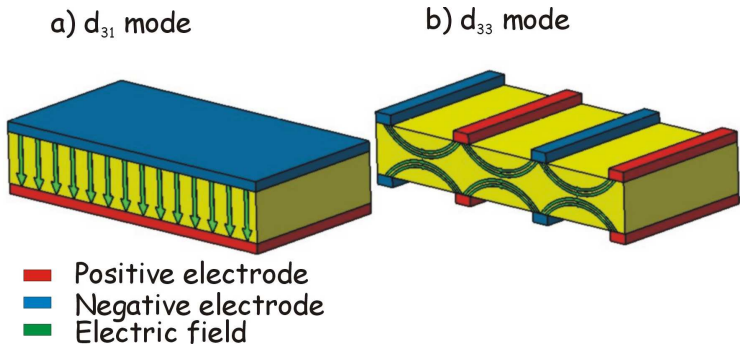

Figure 2: Electric field distribution for different electrode configurations

properties. This was the reason for the development of mixing rules for the determination of the equivalent properties of MFCs from the properties of the constituents in [10]. The mixing rules were derived using the uniform field method and compared to numerical results obtained using the method described and discussed in more details here.

In this paper, after introducing the properties of homogeneous piezoelectric active layers under plane stress driven either in the d_{31} or the d_{33} mode, we develop a numerical method for the evaluation of the equivalent mechanical, piezoelectric and dielectric properties of piezocomposite transducers. The method is based on numerical periodic homogenization performed on a representative volume element (RVE) using three-dimensionnal coupled piezoelectric finite elements. It differs from the methods generally presented in the literature (see for example [24, 20]) in three aspects: (i) the real electrode configuration and the resulting equipotential conditions are taken into account in the RVE, (ii) the peridocicity condition is enforced only in the plane of the transducer, due to the size of the fibers which is of the same order of magnitude as the thickness of the transducer, and (iii) the poling vector is not constant in the RVE and follows the potentially curved electric field lines resulting from the real electrodes configuration.

The method is applied to both d_{31} and d_{33} MFCs with different volume fractions of fibers and the results are compared to the analytical results using the mixing rules developed in [10]. For d_{33} MFCs, the influence of the curved electric field lines as well as the direction of polarization vector on the homogeneous properties are discussed in details.

1.2. Constitutive equations of piezocomposite transducers

Using the standard IEEE notations for linear piezoelectricity, the constitutive equations for an orthotropic piezoelectric material are given by:

$$\begin{Bmatrix} T_1 \\ T_2 \\ T_3 \\ T_4 \\ T_5 \\ T_6 \\ D_1 \\ D_2 \\ D_3 \end{Bmatrix} = \begin{bmatrix} c_{11}^E & c_{12}^E & c_{13}^E & 0 & 0 & 0 & 0 & 0 & -e_{31} \\ c_{12}^E & c_{22}^E & c_{23}^E & 0 & 0 & 0 & 0 & 0 & -e_{32} \\ c_{13}^E & c_{23}^E & c_{33}^E & 0 & 0 & 0 & 0 & 0 & -e_{33} \\ 0 & 0 & 0 & c_{44}^E & 0 & 0 & 0 & -e_{24} & 0 \\ 0 & 0 & 0 & 0 & c_{55}^E & 0 & -e_{15} & 0 & 0 \\ 0 & 0 & 0 & 0 & 0 & c_{66}^E & 0 & 0 & 0 \\ 0 & 0 & 0 & 0 & e_{15} & 0 & \varepsilon_{11}^S & 0 & 0 \\ 0 & 0 & 0 & e_{24} & 0 & 0 & 0 & \varepsilon_{22}^S & 0 \\ e_{31} & e_{32} & e_{33} & & 0 & 0 & 0 & 0 & \varepsilon_{33}^S \end{bmatrix} \begin{Bmatrix} S_1 \\ S_2 \\ S_3 \\ S_4 \\ S_5 \\ S_6 \\ E_1 \\ E_2 \\ E_3 \end{Bmatrix} \tag{1}$$

where E_i and D_i are the components of the electric field vector and the electric displacement vector, and T_i and S_i are the components of stress and strain vectors, defined according to:

$$\begin{Bmatrix} T_1 \\ T_2 \\ T_3 \\ T_4 \\ T_5 \\ T_6 \end{Bmatrix} = \begin{Bmatrix} T_{11} \\ T_{22} \\ T_{33} \\ T_{23} \\ T_{13} \\ T_{12} \end{Bmatrix} \qquad \begin{Bmatrix} S_1 \\ S_2 \\ S_3 \\ S_4 \\ S_5 \\ S_6 \end{Bmatrix} = \begin{Bmatrix} S_{11} \\ S_{22} \\ S_{33} \\ 2\,S_{23} \\ 2\,S_{13} \\ 2\,S_{12} \end{Bmatrix} \tag{2}$$

1.2.1. d_{31} - piezocomposites

For d_{31} piezocomposites, the poling direction (conventionally direction 3) is normal to the plane of the patches (Figure 3a) and according to the plane stress assumption $T_3 = 0$. The electric field is assumed to be aligned with the polarization vector ($E_2 = E_1 = 0$). The constitutive equations reduce to:

$$\begin{Bmatrix} T_1 \\ T_2 \\ T_4 \\ T_5 \\ T_6 \\ D_3 \end{Bmatrix} = \begin{bmatrix} c_{11}^{E*} & c_{12}^{E*} & 0 & 0 & 0 & -e_{31}^* \\ c_{12}^{E*} & c_{22}^{E*} & 0 & 0 & 0 & -e_{32}^* \\ 0 & 0 & c_{44}^{E*} & 0 & 0 & 0 \\ 0 & 0 & 0 & c_{55}^{E*} & 0 & 0 \\ 0 & 0 & 0 & 0 & c_{66}^{E*} & 0 \\ e_{31}^* & e_{32}^* & 0 & 0 & 0 & \varepsilon_{33}^{S*} \end{bmatrix} \begin{Bmatrix} S_1 \\ S_2 \\ S_4 \\ S_5 \\ S_6 \\ E_3 \end{Bmatrix} \tag{3}$$

where the superscript * denotes the properties under the plane stress assumption (which are not equal to the properties in 3D). The constitutive equations can be written in a matrix form, separating the mechanical and

the electrical parts:

$$\{T\} = \left[c^{E*}\right]\{S\} - [e^*]^T\{E\}$$
$$\{D\} = [e^*]\{S\} + \left[\varepsilon^{S*}\right]\{E\}$$

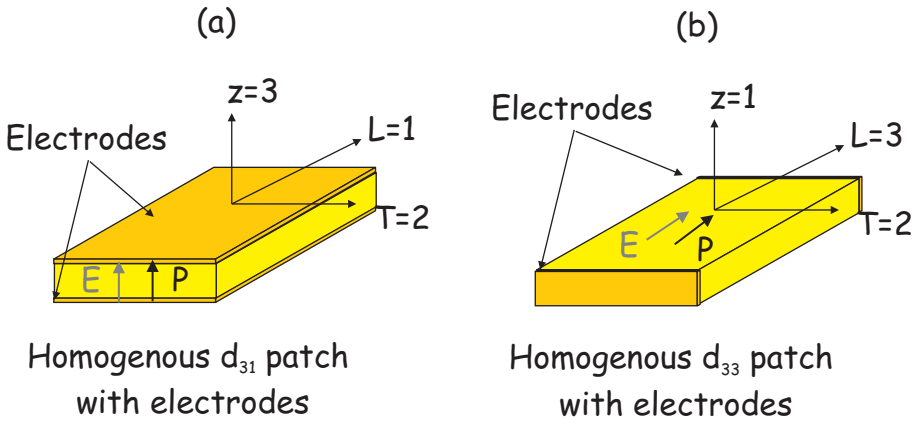

Figure 3: Homogeneous models of the piezoelectric layers with electrodes : d_{31} and d_{33} piezoelectric layers

1.2.2. d_{33} - piezocomposites

For d_{33} piezocomposites, although the electric field lines do not have a constant direction (Figure 2b), when replacing the active layer by an equivalent homogeneous layer, we consider that the poling direction is that of the fibers (direction 3, Figure 3b), and that the electric field is in the same direction. With this reference frame, the plane stress hypothesis implies that $T_1 = 0$. The constitutive equations are given by

$$\begin{Bmatrix} T_2 \\ T_3 \\ T_4 \\ T_5 \\ T_6 \\ D_3 \end{Bmatrix} = \begin{bmatrix} c_{22}^{E*} & c_{23}^{E*} & 0 & 0 & 0 & -e_{32}^* \\ c_{32}^{E*} & c_{33}^{E*} & 0 & 0 & 0 & -e_{33}^* \\ 0 & 0 & c_{44}^{E*} & 0 & 0 & 0 \\ 0 & 0 & 0 & c_{55}^{E*} & 0 & 0 \\ 0 & 0 & 0 & 0 & c_{66}^{E*} & 0 \\ e_{32}^* & e_{33}^* & 0 & 0 & 0 & \varepsilon_{33}^{S*} \end{bmatrix} \begin{Bmatrix} S_2 \\ S_3 \\ S_4 \\ S_5 \\ S_6 \\ E_3 \end{Bmatrix} \tag{4}$$

For both types of piezocomposites, matrix $\left[c^{E*}\right]$ is a function of the longitudinal (in the direction of the fibers) and transverse in-plane Young's moduli (E_L and E_T), the in plane Poisson's ratio ν_{LT}, the in-plane shear modulus

G_{LT}, and the two out-of-plane shear moduli G_{Lz} and G_{Tz}. Matrix $[e^*]$ is given by

$$[e^*] = [d]\left[c^{E*}\right] \tag{5}$$

where

$$[d] = \left[\begin{array}{ccccc} d_{31} & d_{32} & 0 & 0 & 0 \end{array}\right] \tag{6}$$

in the case of d_{31} piezocomposites and

$$[d] = \left[\begin{array}{ccccc} d_{32} & d_{33} & 0 & 0 & 0 \end{array}\right] \tag{7}$$

in the case of d_{33} piezocomposites. Note that the coefficients d_{ij} are unchanged under the plane stress hypothesis.

2. Numerical evaluation of equivalent properties of piezocomposites

Homogenization techniques are widely used in composite materials. They consist in computing the homogeneous, equivalent properties of multi-phase heterogeneous materials. An example of a 1-3 composite is shown on Figure 4 (1-3 refers to the fact that the fibers are connected in one direction and the matrix in all 3 directions). The material is a periodic repetition in all three directions of a so-called representative volume element (RVE) also shown in the figure.

Equivalent properties are obtained by writing the constitutive equations (Equation (3) or (4) in this case) in terms of the average values of T_i, S_i, D_i, E_i on the RVE:

$$\begin{aligned} \overline{T_i} &= \frac{1}{V}\int_V T_i dV \qquad & \overline{D_i} &= \frac{1}{V}\int_V D_i dV \\ \overline{S_i} &= \frac{1}{V}\int_V S_i dV \qquad & \overline{E_i} &= \frac{1}{V}\int_V E_i dV \end{aligned} \tag{8}$$

where $\overline{\ }$ denotes the average value.

A tremendous amount of literature exists on homogenization of elastic and inelastic materials [11, 12, 13]. Extensions have also been made to elastic piezoelectric materials in [14, 15, 16, 17, 18, 19] where analytical results

have been developed. The difficulty with analytical approaches is that they are often restricted to particular geometries (circular or elliptical fibers) and do not take into account complicated electrode patterns such as interdigitated electrodes. The use of numerical approaches such as the finite element method allows to overcome this problem. The principle consists in meshing the RVE and computing approximations of the solution on this RVE using numerical techniques. To our knowledge, this technique has only been applied for Active Fiber Composites (AFC) actuated in the d_{33}-mode. In the model of the RVE, some simplifying assumptions are often made. The first one consists in applying a uniform electric field instead of the real curved electric field [20, 21]. The second one consists in considering that the poling direction is uniform and in the fiber direction [22]. Both these aspects have been taken into account recently in [23] for the evaluation of stress concentration in AFCs, but no homogenization was performed. In addition, the hypothesis that the faces of the RVE remain plane is also often made. The first problem related with this hypothesis is that it results in a large overestimation of the shear stiffness constants. The second problem is that it is not representative of the fact that these transducers are periodic only in two directions (in the plane of the actuator).

The method developed in this paper is inspired from [24] but, due to the specificities of MFC transducers, and the remarks formulated above, differs in the following points: (i) we consider periodicity only in the plane of the actuator, since the thickness of the rectangular fibers is of the same order of magnitude as the thickness of the transducer, (ii) the electrodes are modeled in the RVE (Figure 5), and the macro variable V representing the voltage difference across the electrodes is used instead of the electric field, resulting in additional electrical equipotential conditions, as well as curved electric field lines in the case of d_{33} MFCs, (iii) the poling direction is not necessarily aligned in the direction of the fibers, but follows the electric field lines imposed by the electrodes configuration. Note that a MFC contains more than fifty fibers so that it can be considered as periodic in the direction perpendicular to the fibres.

2.1. Finite element based periodic homogenization of MFCs

When used as sensors or actuators, piezocomposite transducers are typically equipped with two electrodes. These electrodes impose an equipotential

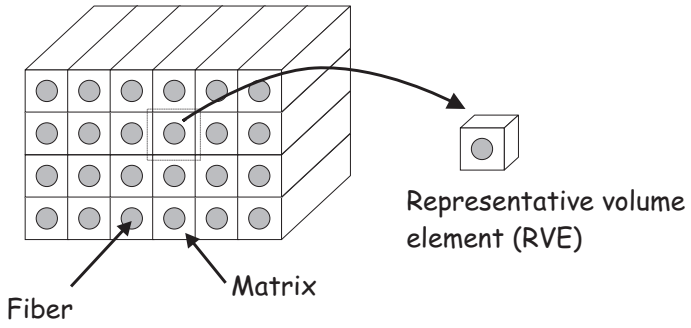

Figure 4: Example of a 1-3 composite and its representative volume element (RVE)

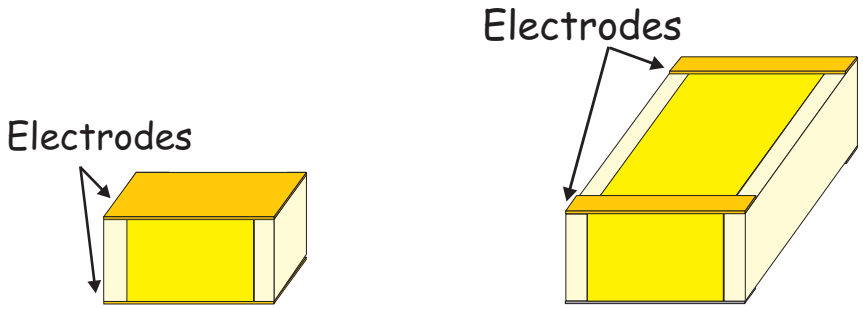

Figure 5: Representative volume element (RVE) for a d_{31} and a d_{33} MFC including the electrodes

voltage on their surfaces, and the electrical variables are the voltage difference V across the electrodes, and the electrical charge Q. These two variables are representative of the electrical macro variables which will be used in the numerical models of structures equipped with such transducers: transducers are used either in open-circuit conditions ($Q = 0$ or imposed) or short-circuit conditions ($V = 0$ or imposed). Instead of the average values of D_i and E_i, the macro variables Q and V are therefore used in the homogenization process. For a homogeneous d_{33} transducer (Figure 6), the constitutive equations can be rewritten in terms of these macro variables:

$$\begin{Bmatrix} T_2 \\ T_3 \\ T_4 \\ T_5 \\ T_6 \\ Q \end{Bmatrix} = \begin{bmatrix} c_{22}^{(SC*)} & c_{23}^{(SC*)} & 0 & 0 & 0 & -e_{32}^*/p \\ c_{32}^{(SC*)} & c_{33}^{(SC*)} & 0 & 0 & 0 & -e_{33}^*/p \\ 0 & 0 & c_{44}^{(SC*)} & 0 & 0 & 0 \\ 0 & 0 & 0 & c_{55}^{(SC*)} & 0 & 0 \\ 0 & 0 & 0 & 0 & c_{66}^{(SC)*} & 0 \\ e_{32}^*A & e_{33}^*A & 0 & 0 & 0 & \varepsilon_{33}^{s*}A/p \end{bmatrix} \begin{Bmatrix} S_2 \\ S_3 \\ S_4 \\ S_5 \\ S_6 \\ -V \end{Bmatrix} \tag{9}$$

where SC stands for 'short-circuit' ($V = 0$), p is the length of the transducer, A is the surface of the electrodes of the equivalent homogeneous transducer and Q is the charge collected on the electrodes.

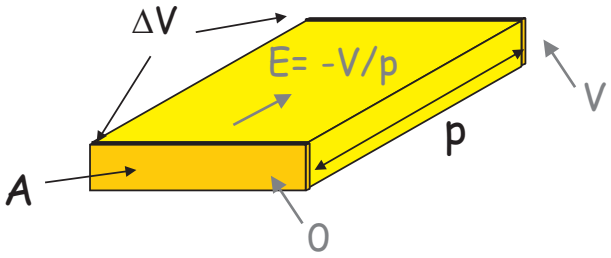

Figure 6: Homogeneous model of the d_{33} piezocomposite and definition of the macro variables

For d_{31}-piezocomposites, the approach is identical.

2.1.1. Definition of local problems

The RVE is made of two different materials. In order to find the homogeneous constitutive equations, Equation (9) is written in terms of the average

values of the mechanical quantities S_i and T_i in the RVE and the electrical variables Q and V defined on the electrodes:

$$\begin{Bmatrix} \overline{T_2} \\ \overline{T_3} \\ \overline{T_4} \\ \overline{T_5} \\ \overline{T_6} \\ Q \end{Bmatrix} = \begin{bmatrix} \overline{c_{22}}^{(SC*)} & \overline{c_{23}}^{(SC*)} & 0 & 0 & 0 & -\overline{e_{32}}^{*}/p \\ \overline{c_{32}}^{(SC*)} & \overline{c_{33}}^{(SC*)} & 0 & 0 & 0 & -\overline{e_{33}}^{*}/p \\ 0 & 0 & \overline{c_{44}}^{(SC*)} & 0 & 0 & 0 \\ 0 & 0 & 0 & \overline{c_{55}}^{(SC*)} & 0 & 0 \\ 0 & 0 & 0 & 0 & \overline{c_{66}}^{(SC*)} & 0 \\ \overline{e_{32}}^{*}A & \overline{e_{33}}^{*}A & 0 & 0 & 0 & \overline{\varepsilon_{33}}^{S*}A/p \end{bmatrix} \begin{Bmatrix} \overline{S_2} \\ \overline{S_3} \\ \overline{S_4} \\ \overline{S_5} \\ \overline{S_6} \\ -V \end{Bmatrix} \tag{10}$$

The different terms in Equation (10) can be identified by defining local problems on the RVE. The technique consists in imposing conditions on the different strain components and V and computing the average values of the stress and the charge in order to find the different coefficients. For the electric potential, two different conditions ($V = 0, 1$) are used. For the mechanical part, we assume that the displacement field is periodic in the plane of the transducer (see i.e [24]): on the boundary of the RVE (but not on the upper and lower surfaces since the piezocomposite is not periodic in that direction), the displacement can be written:

$$u_i = \overline{S}_{ij}\, x_j + v_i \tag{11}$$

where u_i is the i^{th} component of displacement, $\overline{S}_{ij}$ is the average strain in the RVE (tensorial notations are used), x_j is the j^{th} spatial coordinate of the point considered on the boundary, and v_i is the periodic fluctuation on the RVE. The fluctuation v is periodic in the plane of the transducer so that between two opposite faces (noted B^-/B^+ and C^-/C^+, Figure 7), one can write ($v(x_j^{K+}) = v(x_j^{K-})$, $K = B, C$):

$$u_i^{K+} - u_i^{K-} = \overline{S}_{ij}\,(x_j^{K+} - x_j^{K-}) \qquad K = B, C \tag{12}$$

For a given value of the average strain tensor ($\overline{S}_{ij}$), Equation (12) defines constraints between the points on each pair of opposite faces. This is illustrated in Figure 8, where an average strain S_2 is imposed on the RVE and the constraints are represented for u_2 on faces B^- and B^+.

Note that these constraints do not impose that the faces of the RVE remain plane, which is important for the evaluation of the shear stiffness

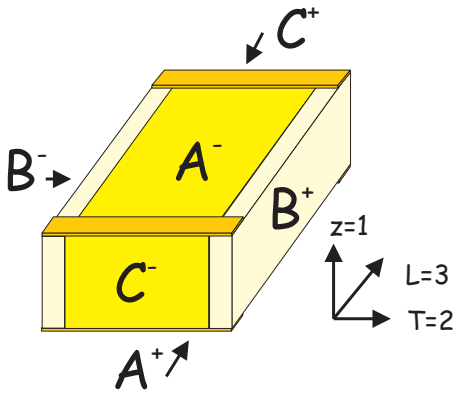

Figure 7: Definition of pairs of opposite faces on the RVE

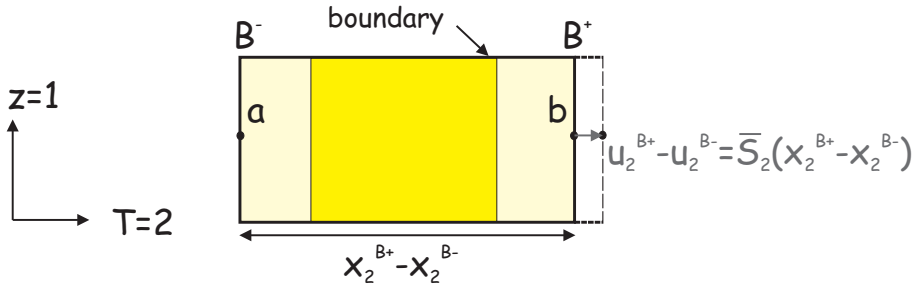

Figure 8: Example of an average strain S_2 imposed on the RVE and associated periodic conditions

coefficients. For faces A^- and A^+, the displacement is unconstrained in the normal direction, because the MFC is not periodic in this direction.

In total, six local problems are needed to identify all the coefficients in (10) (Figure 9). The first problem consists in applying a difference of potential V to the electrodes of the RVE and imposing zero displacement on all the faces (except the top and bottom). The deformed mesh resulting from the finite element computation for this local problem is represented in Figure 10 for a d_{31}-MFC. In the next five local problems, the difference of potential is set to 0 (short-circuited condition), and five deformation mechanisms are induced. Each of the deformation mechanisms consists in a unitary strain in one of the directions (with zero strain in all the other directions). For each case, the average values of T_i and S_i, and the charge accumulated on the electrodes Q, are computed, and used to determine all the coefficients in (10), from which the engineering constants are determined. Note that the electrodes are included in a particular layer which is in direct contact with the active layer considered for homogenization, so that they are modeled as an electrical boundary condition on the RVE only. The mechanical properties of the electrodes should be taken into account when modeling the full MFC, as detailed in [10].

2.2. Comparison with the analytical mixing rules

2.2.1. d_{31} MFCs

The homogeneous properties of d_{31}-MFCs have been computed for different volume fractions between $\rho = 0$ and $\rho = 1$ (bulk ceramic) using the mixing rules developed in [10] and the numerical method presented in section 2.1. A comparison with experimental results would also be very useful but MFC properties have only been measured for a single volume fraction of fibers ($\rho = 0.86$). A comparison with these measurements can be found in [10].

The properties of the fibers are given in Table 1 (it is assumed that the fibers are made of SONOX P502 from $CeramTec$, direction 3 is the poling direction. For more details, see [25]). For the matrix, typical values for epoxy are considered: $E = 2.9GPa$, $\nu = 0.3$ and $\varepsilon_{11}^T/\varepsilon_0 = \varepsilon_{22}^T/\varepsilon_0 = \varepsilon_{33}^T/\varepsilon_0 = 4.25$.

The evolution of the different mechanical, piezoelectric and dielectric properties as a function of the fiber volume fraction is represented on Figures 11 and 12. Direction L corresponds to the fiber direction, T is the

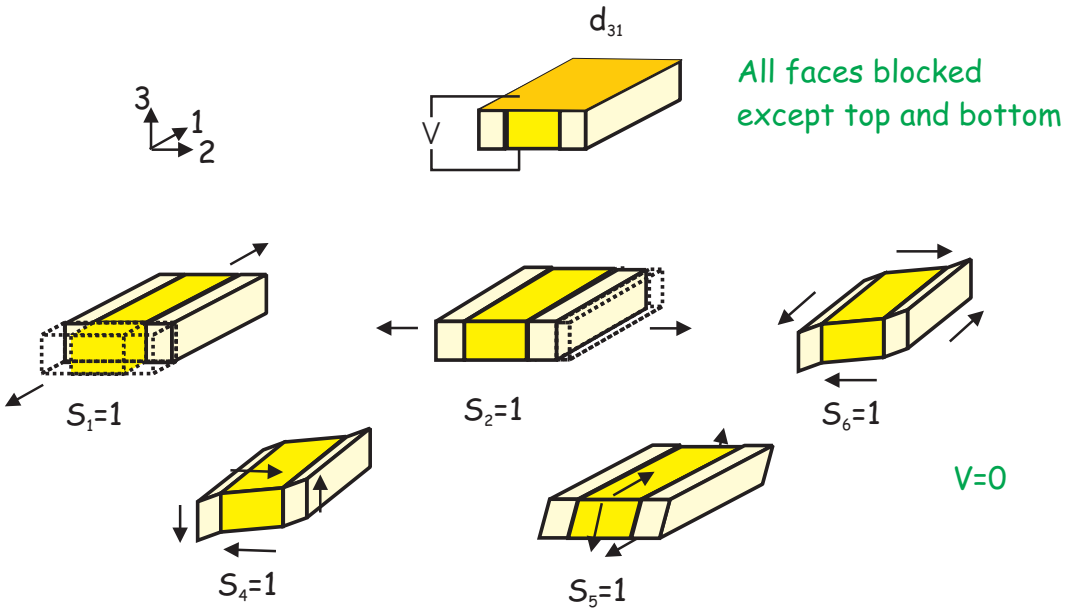

Figure 9: The six local problems solved by the finite element method in order to compute the homogenized properties of d_{31}-MFCs

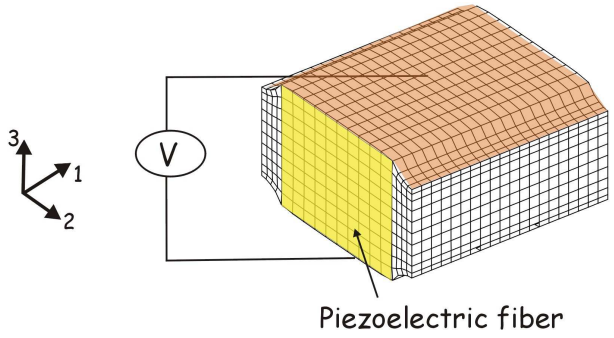

Figure 10: Deformation of the RVE of a d_{31}-MFC under applied electric potential difference V between the top and bottom electrodes computed using finite element 3D piezoelectric elements. All faces are fixed except top and bottom (fiber volume fraction $\rho = 0.9$).

MFC Fiber Engineering constants	Symbol	Unit	SONOX P502 (set 1)
Young's modulus	$E_1 = E_2$	GPa	54.05
	E_3	GPa	48.30
Shear modulus	$G_{23} = G_{31}$	GPa	19.48
	G_{12}	GPa	19.14
Poisson's ratio	$\nu_{23} = \nu_{13}$	-	0.44
	ν_{12}	-	0.41
Piezoelectric charge constants	$d_{32} = d_{31}$	pC/N	-185
	d_{33}	pC/N	440
	$d_{15} = d_{24}$	pC/N	560
Dieletric relative constants (free)	$\varepsilon_{11}^T/\varepsilon_0 = \varepsilon_{22}^T/\varepsilon_0$	-	1950
	$\varepsilon_{33}^T/\varepsilon_0$	-	1850

Table 1: MFC fibers engineering constants

transverse direction, and z is the out-of-plane direction.

For the mechanical properties, the match is very good for E_L, E_T, G_{LT} and ν_{LT}. For G_{Lz} and G_{Tz}, the numerical results are higher, especially for high volume fractions of fibers. This is due to the presence of an inhomogeneous electric field in the Lz plane, mainly in the L direction for G_{Lz}, and in the Tz plane, mainly in the T direction for G_{Tz} (Figure 13). If zero electric potential was imposed on all the faces of the RVE instead of the real short-circuit conditions (this is done for example in [24, 20, 21]), these electric fields would not be present and there would be no stiffening of the piezocomposite for high volume fractions. This corresponds to the hypothesis made in the uniform field method (UFM) used to derive the mixing rules. Imposing zero potential on the actual electrodes only, leads therefore to interesting results different from the ones traditionally found in the literature.

For the piezoelectric properties, the match is very good for d_{31}, and good for d_{32} despite of a larger discrepancy for low volume fractions. Note however that the match is good for e_{31} and e_{32} which are most often used in shell finite element formulations. The difference between the mixing rules and the numerical approach is due to the inhomogeneity of the different fields

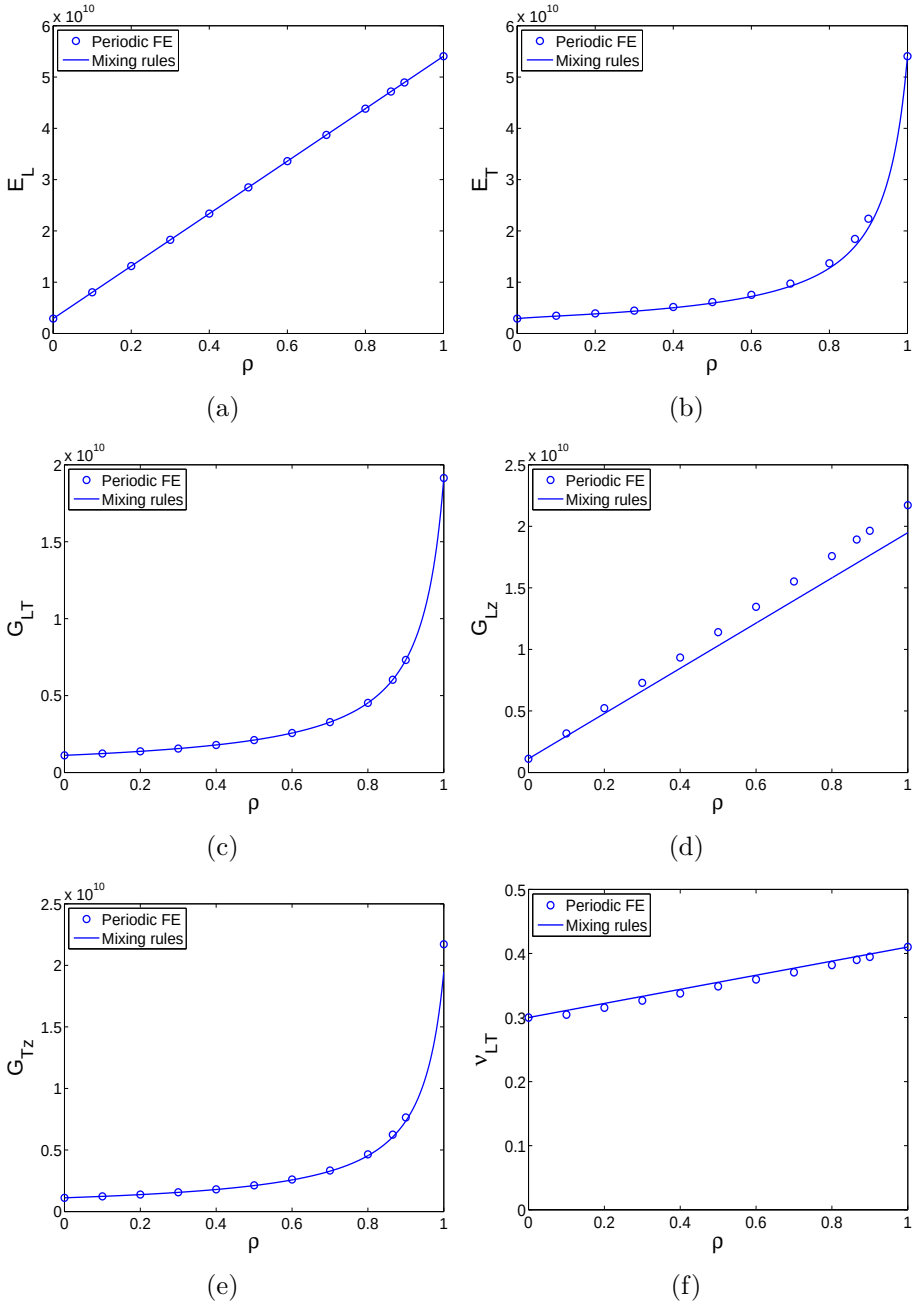

Figure 11: Evolution of the mechanical properties of d_{31} MFCs as a function of the fiber volume fraction: comparison between the mixing rules and periodic finite element homogenization

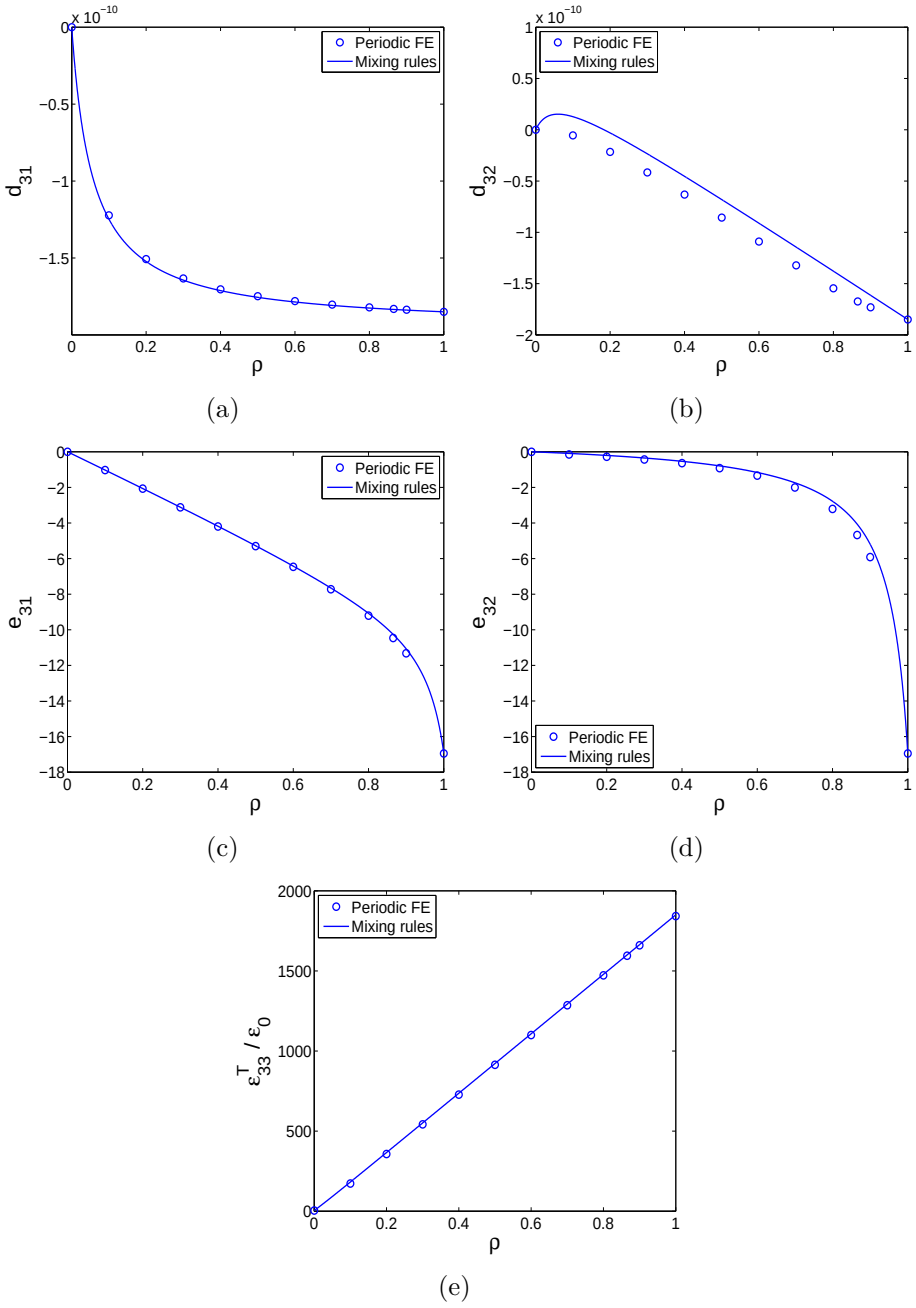

Figure 12: Evolution of piezoelectric and dielectric properties of d_{31} MFCs as a function of the fiber volume fraction: comparison between the mixing rules and periodic finite element homogenization

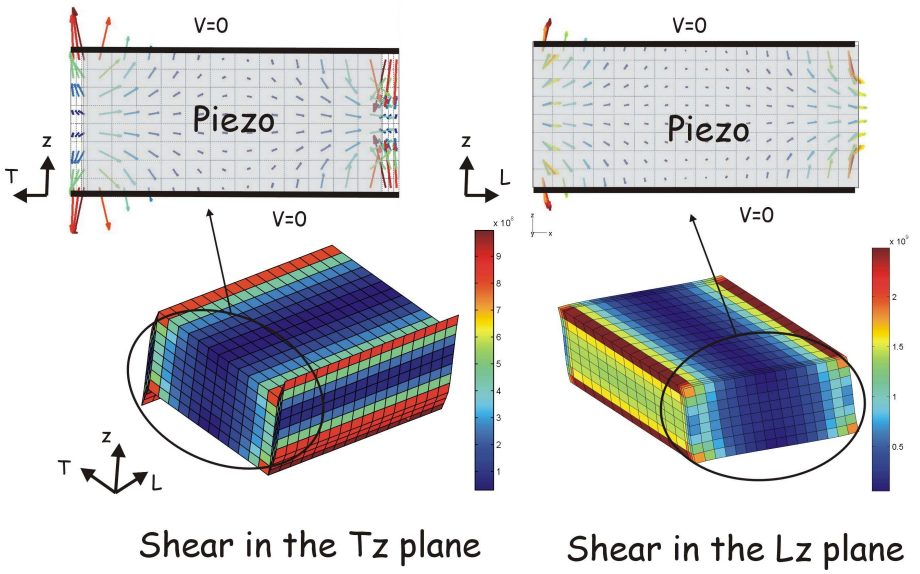

Figure 13: Electric fields in the piezocomposite due to a shear strain in short-circuited conditions. RVE with $\rho = 0.9$

in the finite element approach. It has been found that this inhomogeneity comes mainly from the plane stress assumption which results in deformed shapes of the kind reported in Figure 14, where one sees that the out-of-plane stresses and strains are not uniform in the fiber and the matrix. Note that this analysis is different from the one presented in [25] where the fields were much more uniform because the periodicity conditions was imposed in the direction perpendicular to the plane of the actuator.

2.2.2. d_{33} MFCs

The RVE used for the periodic finite element homogenization is shown in Figure 15. It includes the definition of the interdigitated electrodes. The length of the RVE (p), corresponding to the distance between the finger electrodes, is 6 times the thickness h of the transducer (for a study of the influence of this ratio, see [1]) and the width of the electrodes is equal to this thickness. In a first study, it is assumed that the poling direction is parallel to the fiber direction. This hypothesis will be further discussed in section 2.2.3.

The evolution of the different mechanical, piezoelectric and dielectric

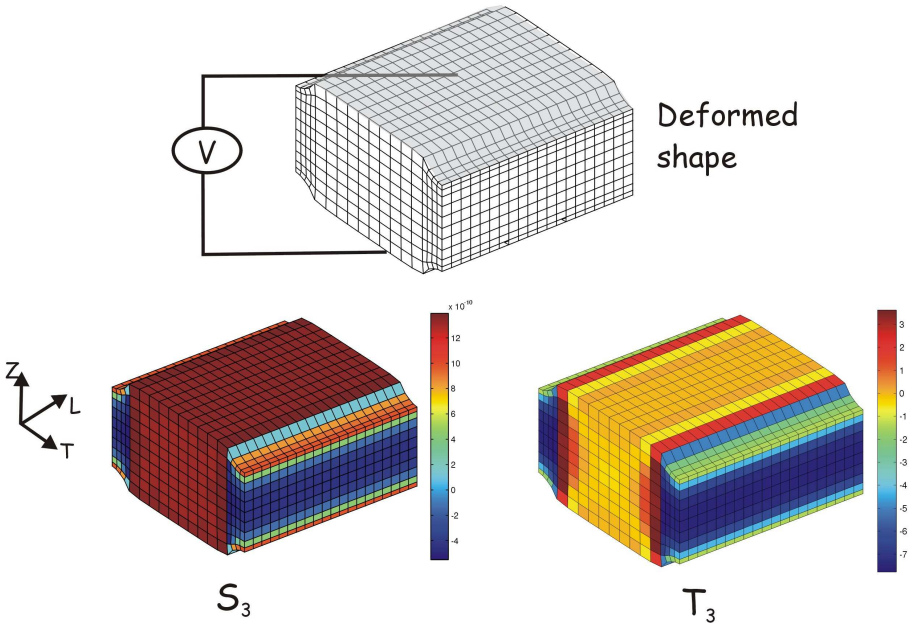

Figure 14: Deformed shaped under the plane stress assumption when an electric potential diffierence is applied to the electrodes. The out-of-plane stresses and strains are not uniform. RVE with $\rho = 0.9$

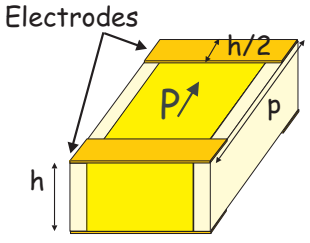

Figure 15: Representative volume element (RVE), p/h=6

properties as a function of the fiber volume fraction is represented in Figures 16 and 17 where they are compared with the analytical mixing rules.

For the mechanical properties, the match is good, but there is a stiffening for the longitudinal modulus and the two shear moduli G_{Lz} and G_{Tz} for high volume fractions of PZT. This is due to the presence of an electric field in the composite in short-circuited conditions (Figure 18, similar to what was observed for d_{31}-MFCs). It is interesting to note that for the shear moduli, the stiffening is stronger than in the case of d_{31}-MFCs. This is due to the fact that the electrode is not continuous on the top and bottom faces, so that a stronger and more homogeneous electric field can develop in the region between the electrodes. For the longitudinal modulus, the appearance of the electric field is due to the existence of curved electric field lines.

For the piezoelectric properties, the match is good for e_{31} and e_{32}. The values of d_{32} and d_{33} are slightly lower than the values computed using the mixing rules. This effect is directly related to the stiffening of the piezocomposite in the longitudinal direction due to the presence of electric fields in short-circuited conditions.

Another interesting remark is that the free strain is not uniform (Figure 19). In the region below the electrodes, the electric field is not aligned with the poling direction and changes direction and magnitude quickly. The average induced stress is however equivalent to an ideal d_{33} actuator for which $E_3 = -V/p$. This is because the value of the electric field in the region between the electrodes has been found to be approximately equal to $E_3 = -V/(p-h)$ so that it is stronger than for the ideal d_{33} (for which $E_3 = -V/p$) and compensates for the inactive zone below the electrodes.

2.2.3. Influence of the poling direction for d_{33} MFCs

Figure 20 shows the amplitude and direction of the electric field for a d_{33}-MFC ($\rho = 0.9$) resulting from the application of a potential difference on the interdigitated electrodes. During the manufacturing, the poling of the piezoelectric fibers is done by imposing very high electric fields to the interdigitated electrodes. This results in a poling direction aligned with the applied electric field. The hypothesis that the poling direction is in the fiber direction is therefore only valid in the region between the finger electrodes.

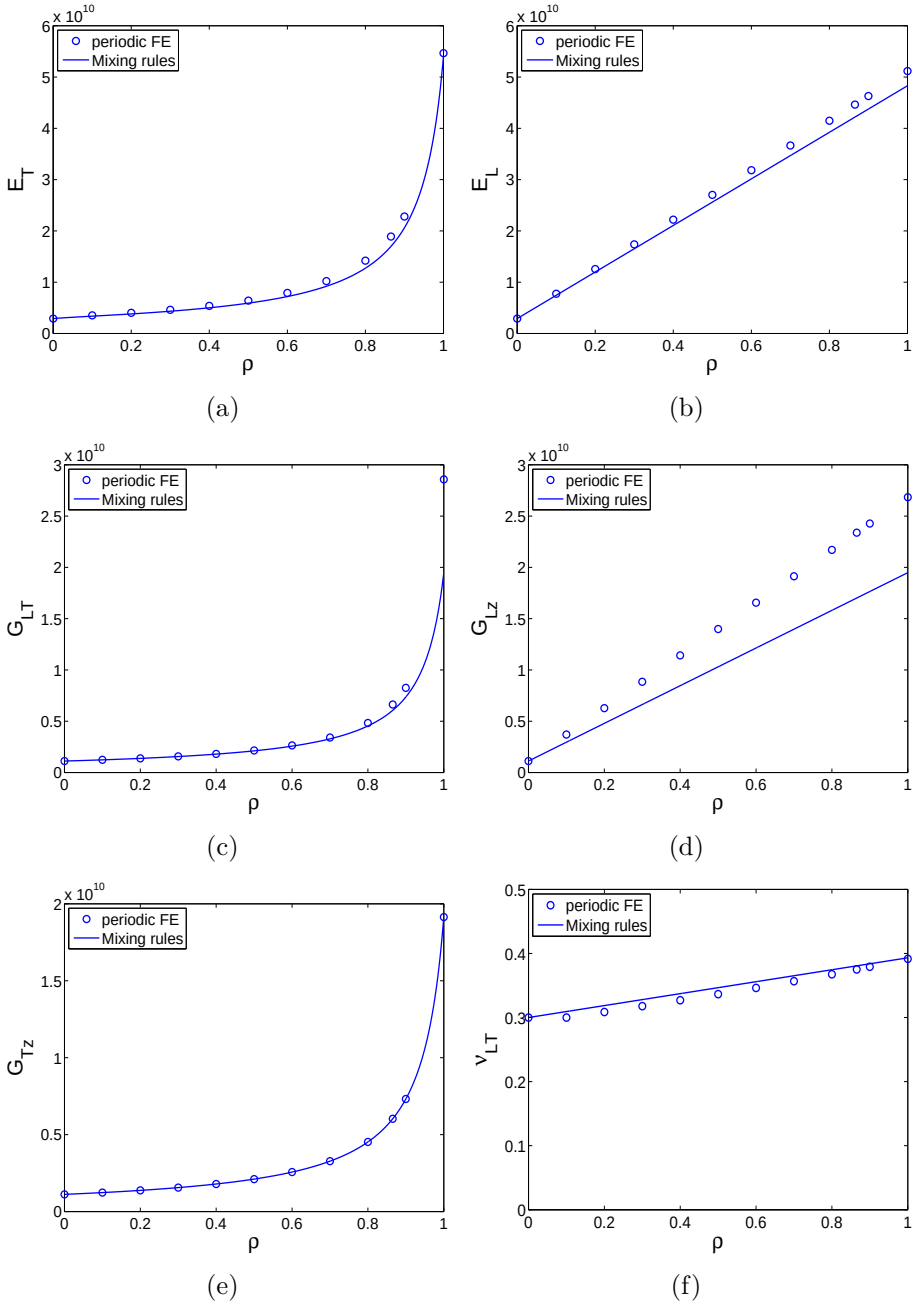

Figure 16: Evolution of the mechanical properties of d_{33} MFCs as a function of the fiber volume fraction: comparison between the mixing rules and periodic finite element homogenization

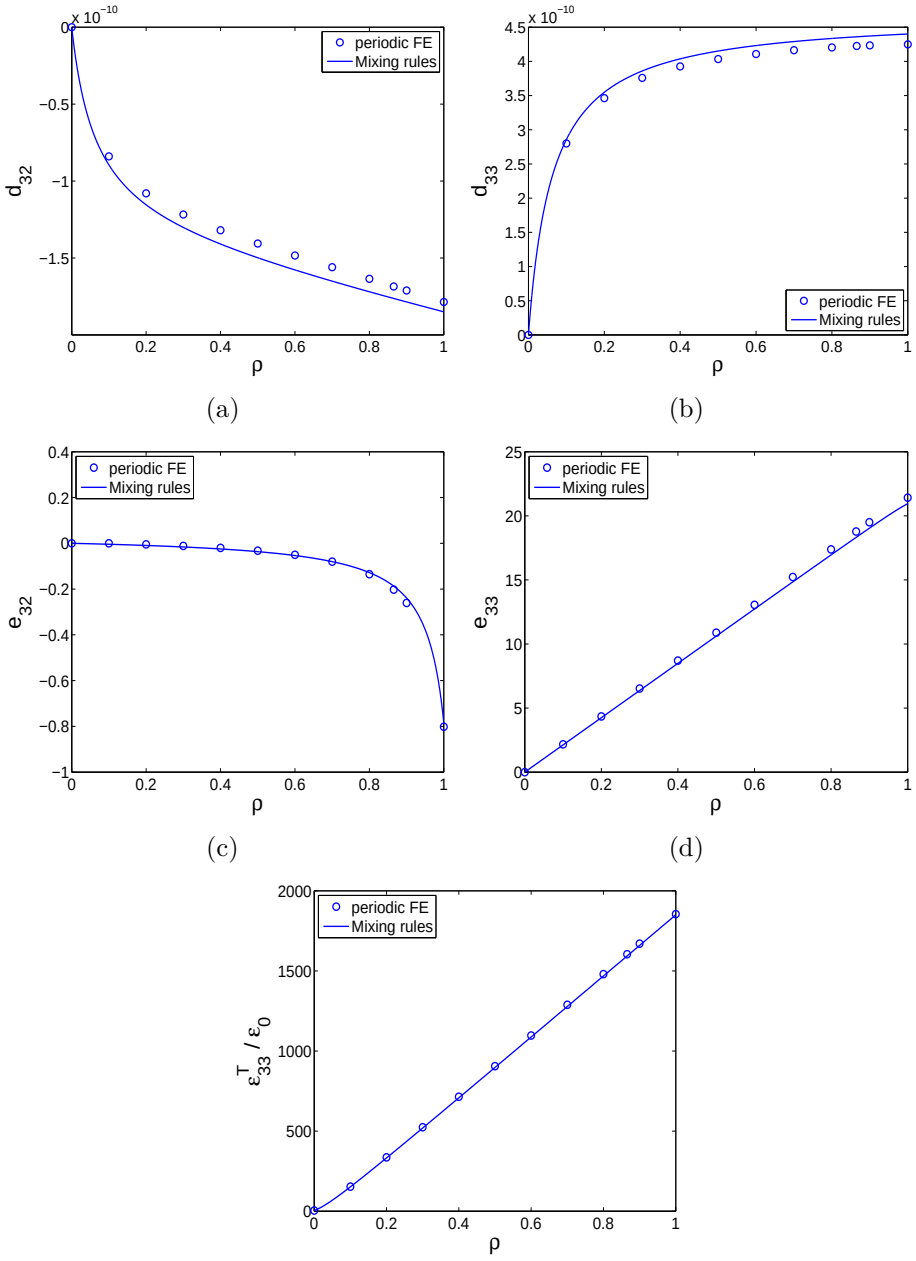

Figure 17: Evolution of piezoelectric and dielectric properties of d_{33} MFCs as a function of the fiber volume fraction: comparison between the mixing rules and periodic finite element homogenization

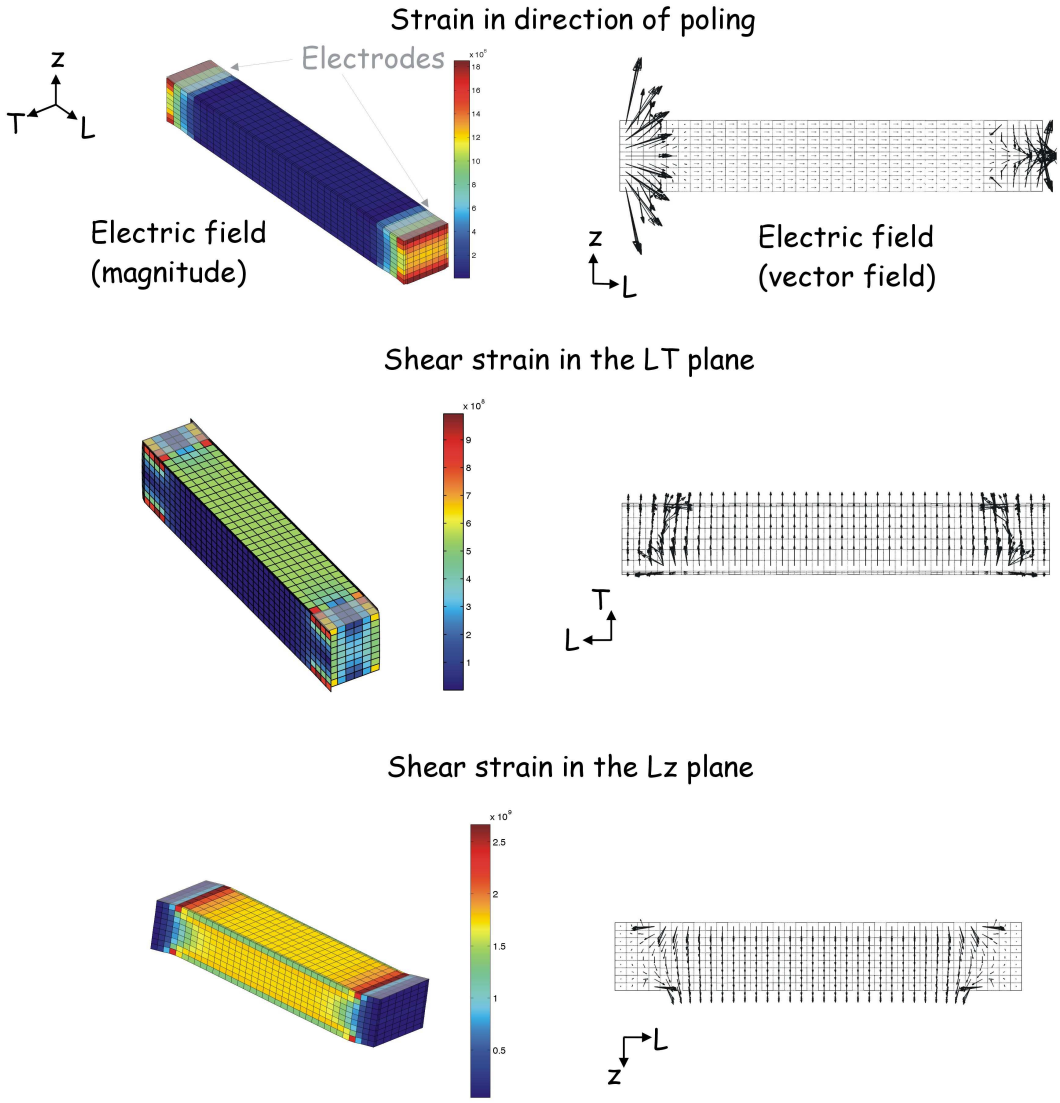

Figure 18: Electric fields in the piezocomposite due to a longitudinal strain and shear strains in short-circuited conditions. RVE with $\rho = 0.9$

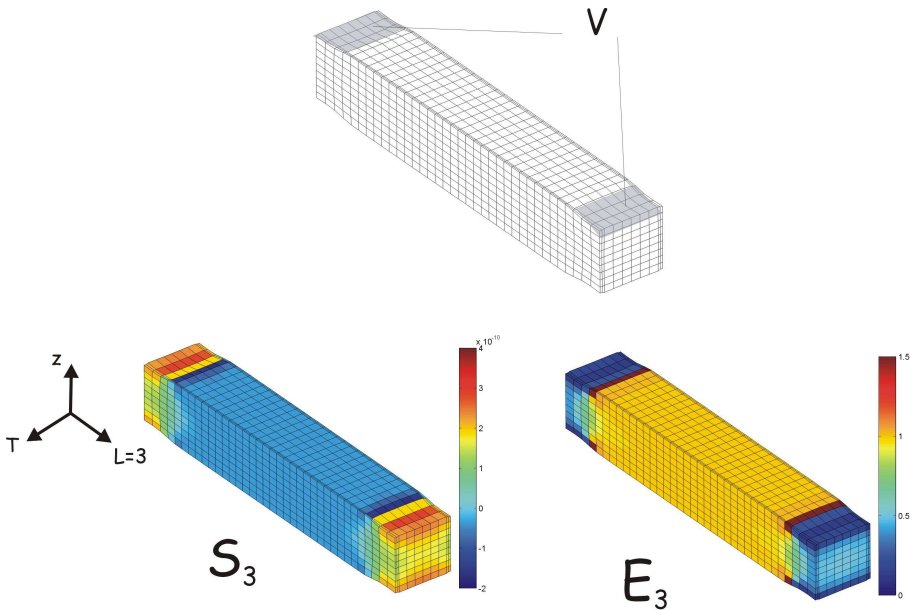

Figure 19: Induced strain S_3 and electric field E_3 due to the application of a potential difference V. RVE with $\rho = 0.9$

In order to take this into account, we have corrected the finite element computations by introducing a local polarization vector in each element which is aligned with the electric field. In a first step, the electric field lines are computed with the poling vector aligned with the fiber direction L. In a second step, the poling direction is adjusted and aligned with the electric field lines as shown in Figure 20. In Figures 21 and 22, we compare the results obtained with the polarization in the direction of the fibers and the polarization aligned with the electric field. The figures show that there is a minor difference due to a stronger stiffening in the longitudinal direction. This is due to an increase in non-zero electric field between the short circuited electrodes when the polarization is aligned with the electric field.

The direction of poling has a small influence on the average behavior of the d_{33} piezocomposite because the regions below the electrodes do not contribute very much to the overall behavior. If one is concerned with more local values such as stress concentrations which occur in the regions below the electrodes, this influence may be important and should be further studied [23].

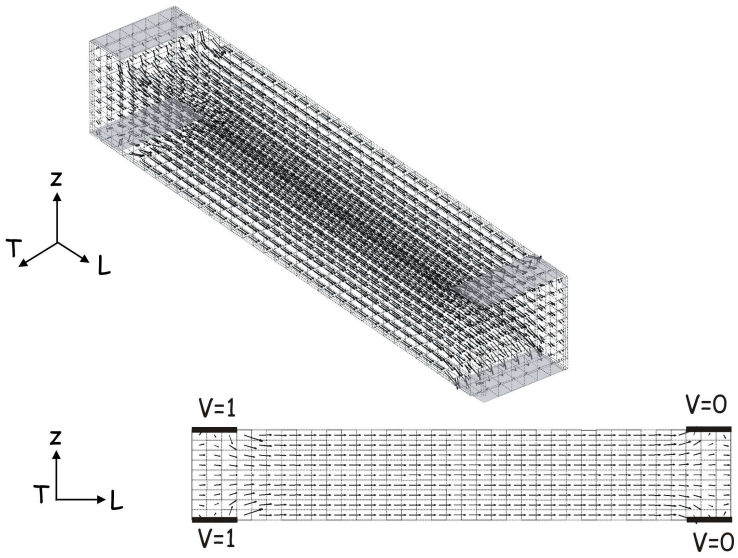

Figure 20: Electric field (direction and amplitude) due to the application of an electrical potential difference V. RVE with $\rho = 0.9$

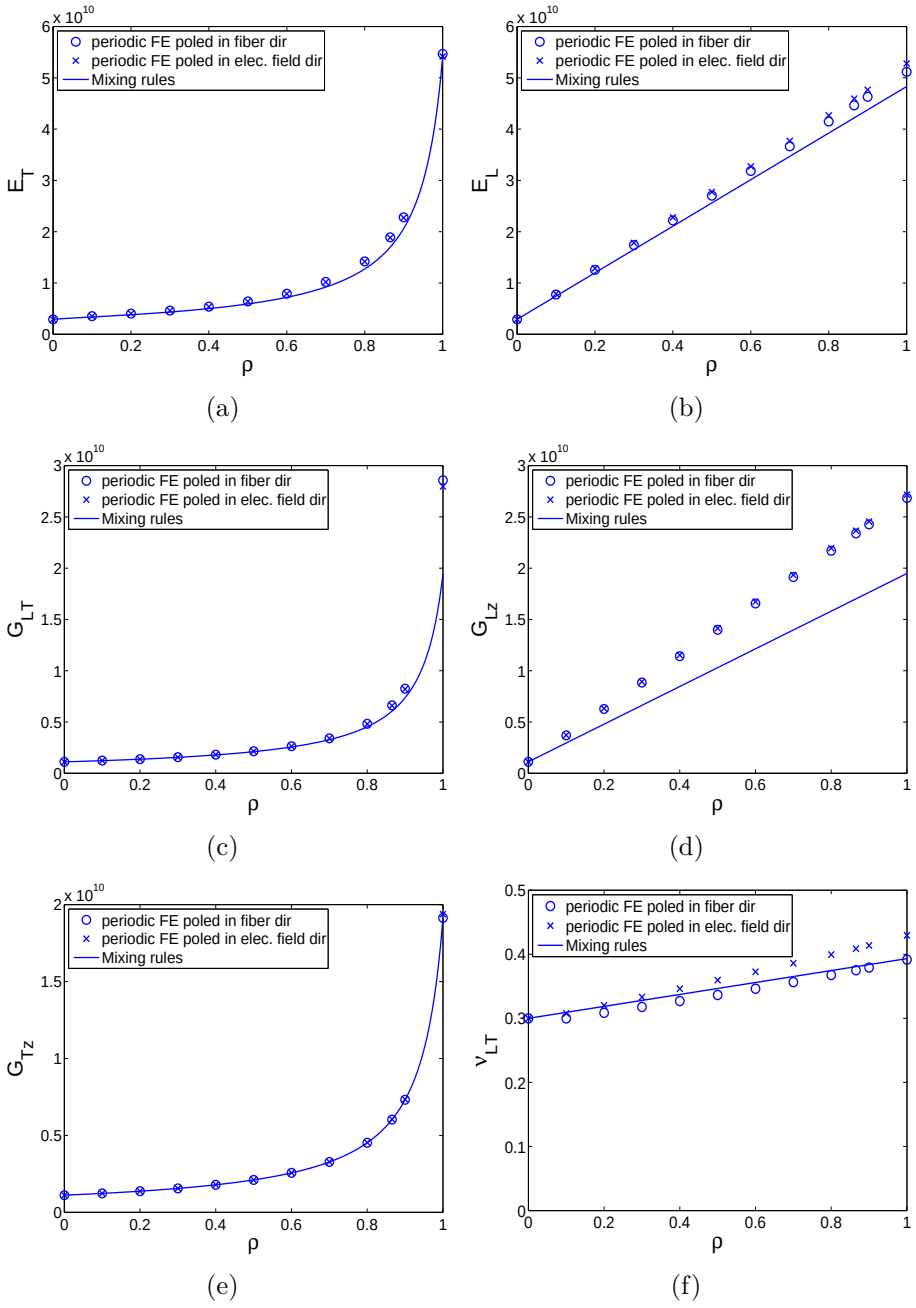

Figure 21: Evolution of the mechanical properties of d_{33} MFCs as a function of the fiber volume fraction: comparison between the mixing rules and periodic finite element homogenization (fibers poled in direction L or aligned with the electric field)

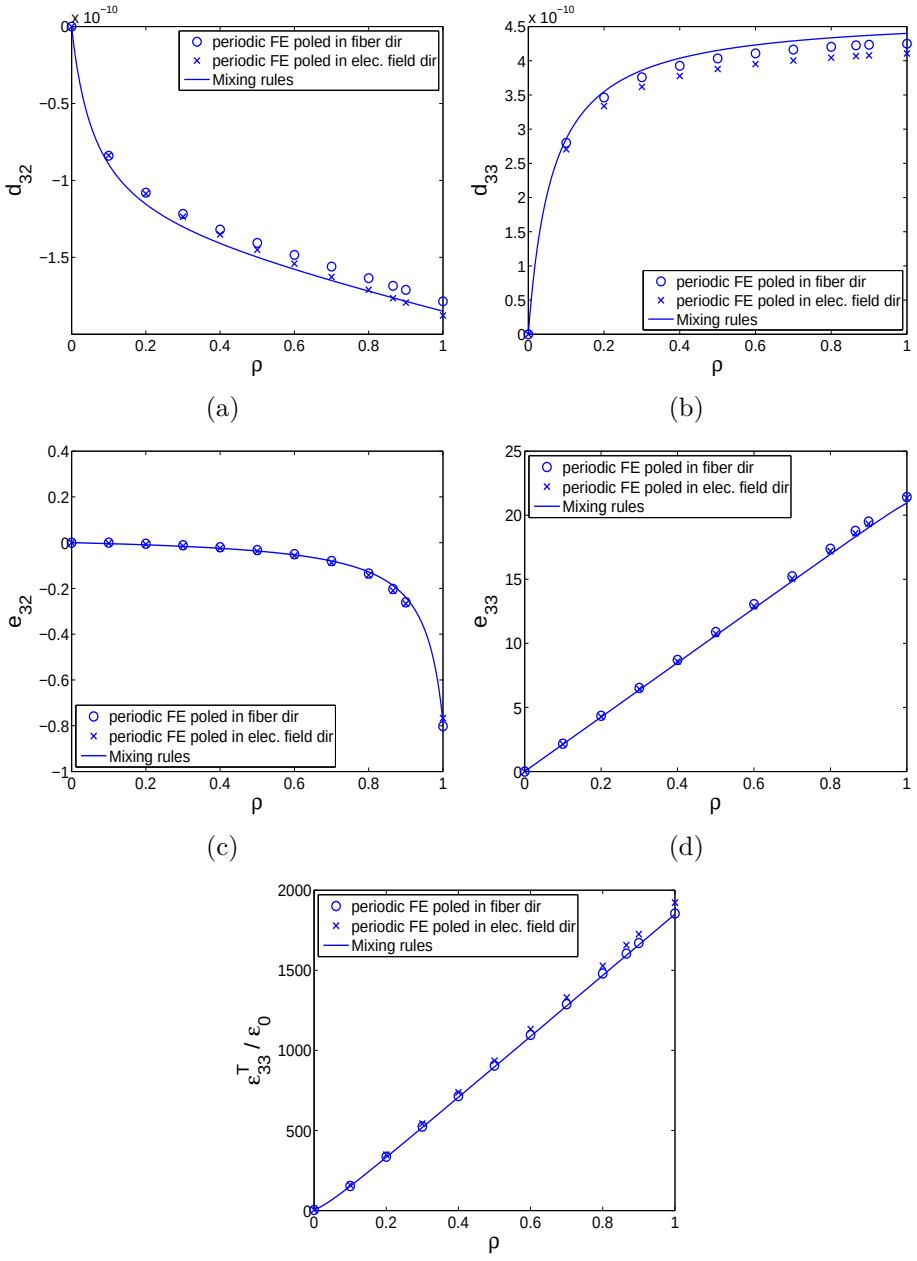

Figure 22: Evolution of piezoelectric and dielectric properties of d_{33} MFCs as a function of the fiber volume fraction: comparison between the mixing rules and periodic finite element homogenization (fibers poled in direction L or aligned with the electric field)

3. Conclusion

In this paper, finite element periodic homogenization has been applied to both d_{31} and d_{33} MFC transducers. The method presented differs from the ones traditionally found in the literature in three main aspects: (i) periodicity is enforced only in the plane of the transducer and not in all three directions, which is more representative of the fact that only one fiber is present through the thickness, (ii) the electrodes are modeled in the RVE, and the macro variables V and Q representing the voltage difference across the electrodes and the charge collected on the electrodes is used instead of the electric field, resulting in additional electrical equipotential conditions, as well as curved electric field lines in the case of d_{33} MFCs, (iii) the poling direction is not necessarily aligned in the direction of the fibers, but follows the electric field lines imposed by the electrodes configuration. The homogeneous properties of both d_{31} and d_{33} MFCs have been computed using this method for different volume fractions of fibers, and compared to previously published analytical mixing rules. Although there is in general a good agreement between the numerical and the analytical results, some differences were found due to: (i) the electrical boundary conditions and the curved electric field lines (in the case of d_{33}-MFCs) imposed by the specific electrodes configuration which are not taken into account in the analytical approach, and (ii) the non uniformity of the stress and strain fields resulting from the release of the periodicity condition in the perpendicular direction. This highlights the importance of correctly modeling the electrodes and performing the homogenization using the macro electrical variables V and Q rather than the local electric fields and electric displacements. For d_{33} MFCs, the influence of the poling direction, either aligned in the fiber direction, or aligned with the electric field lines (which corresponds to the reality for these types of transducers) has been studied. It has been shown that the influence on the homogenized properties was minor, although the influence on some local values (stress concentrations) can be high. The method presented is general and could be applied to other types of piezocomposites than the Macro Fiber Composites treated in this paper.

Acknowledgements

This work was supported in part by the Fond National de la Recherche Luxembourg in the context of the FNR MAFICOMECH Project (C08/MS/17).

References

[1] N. Hagood, R. Kindel, K. Ghandi, P. Gaudenzi, Improving transverse actuation of piezoceramics using interdigitated surface electrodes, in: N. W. Hagood (Ed.), Proc. SPIE Vol. 1917, 1993, pp. 341–352.

[2] K. Lazarus, M. Lundstrom, J. Moore, E. Crawley, Packaged strain actuator, US Patent 5687462.

[3] G. Horner, Piezoelectric composite device and method for making same, International patent application WO0217407.

[4] P. Wierach, Elektromechanisches funktionsmodul, German Patent DE 10051784 C1.

[5] W. Wilkie, R. Bryant, J. High, R. Fox, R. Hellbaum, A. Jalink, B. Little, P. Mirick, Low-cost piezocomposite actuator for structural control applications, in: Proc. SPIE 7th Annual Int. Symp. Smart. Struct. Mater., Newport Beach, USA, 2000.

[6] A. Bent, N. Hagood, J. Rodgers, Anisotropic actuation with piezoelectric fiber composites, J. Intell. Mater. Syst. Struct 6 (1995) 338–349.

[7] P. Wierach, Low profile piezo actuators based on multilayer technology, in: Proc. of 17th Int. Conf. on Adaptive Structures and Technologies (ICAST2006), Taipei, Taiwan, 2006.

[8] B. Williams, G. Park, D. Inman, W. Wilkie, An overview of composite actuators with piezoceramic fibers, in: Proc. of 20th Int. Modal Analysis Conference (IMAC), Los Angeles, USA, 2002.

[9] V. Piefort, Finite element modelling of piezoelectric active structures, Ph.D. thesis, Université Libre de Bruxelles (June 2001).

[10] A. Deraemaeker, H. Nasser, A. Benjeddou, A. Preumont, Mixing rules for the piezoelectric properties of Macro Fiber Composites, J. Intell. Mater. Syst. Struct 20(12) (2009) 1391–1518.

[11] Z. Hashin, S. Shtrikman, On some variational principles in anisotropic and nonhomogeneous elasticity, J. Mech. Phys. Solids 10 (1962) 335–342.

[12] Z. Hashin, S. Shtrikman, A variational approach to the theory of the elastic behaviour of multiphase materials, J. Mech. Phys. Solids 11 (1963) 127–140.

[13] Z. Xia, Y. Zhang, F. Ellyin, A unified periodical boundary conditions for representative volume elements of composites and applications, International Journal of Solids and Structures 40 (2003) 1907–1921.

[14] D. Skinner, R. Newnham, L. Cross, Flexible composite transducers, Mat. Res. Bull. 13 (1978) 599–607.

[15] R. Newnham, D. Skinner, L. Cross, Connectivity and piezoelectric-pyroelectric composites, Mat. Res. Bull. 13 (1978) 525–536.

[16] F. Levassort, M. Lethiecq, D. Certon, F. Patat, A matrix method for modeling electroelastic moduli of 0-3 piezo-composites, IEEE Transactions on Ultrasonics, Ferroelectrics, and Frequency Control 44(2) (1997) 445–452.

[17] M. Dunn, M. Taya, Micromechanics predictions of the effective electroelastic moduli of piezoelectric composites, Int. J. Solids Structures 30(2) (1993) 161–175.

[18] A. Agbossou, C. Richard, Y. Vigier, Segmented piezoelectric fiber composite for vibration control: fabricating and modeling of electromechanical properties, Composites Science and Technology 63 (2003) 871–881.

[19] J. Smay, J. Cesarano, A. Tuttle, J. Lewis, Piezoelectric properties of 3-X periodic Pb(ZrxTi1-x)O3 - polymer composites, Journal of applied physics 92(10) (2002) 6119–6127.

[20] C. Poizat, M. Sester, Effective properties of composites with embedded piezoelectric fibres, Computational Materials Science 16 (1999) 89–97.

[21] E. Lenglet, A. Hladky-Hennion, J. Debus, Numerical homogenization techniques applied to piezoelectric composites, J. Acoust. Soc. Am. 113 (2003) 826–833.

[22] A. Bent, N. Hagood, Piezoelectric fiber composites with interdigitated electrode, J. Intell. Mater. Syst. Struct 8 (1997) 903–919.

[23] R. Paradies, M. Melnykowycz, Numerical stress investigation for piezoelectric elements with a circular cross section and interdigitated electrodes, J. Intell. Mater. Syst. Struct 18 (2007) 963–972.

[24] H. Berger, S. Kari, U. Gabbert, R. Rodriguez-Ramos, J. Bravo-Castillero, R. Guinovart-Diaz, F. J. Sabina, G. A. Maugin, Unit cell models of piezoelectric fiber composites for numerical and analytical calculation of effective properties, Smart Mater. Struct. 15 (2006) 451–458.

[25] A. Deraemaeker, S. Benelechi, A. Benjeddou, A. Preumont, Analytical and numerical computation of homogenized properties of MFCs: Application to a composite boom with MFC actuators and sensors, in: Proc. III ECCOMAS thematic conference on Smart Structures and Materials, Gdansk, Poland, 2007.